Large underground, liquid based detectors for astro-particle physics in Europe: scientific case and prospects

D Autiero [1], J Äystö [2], A Badertscher [3], L Bezrukov [4], J Bouchez [5], A Bueno [6], J Busto [7], J-E Campagne [8], Ch Cavata [9], L Chaussard [1], A de Bellefon [10], Y Déclais [1], J Dumarchez [11], J Ebert [12], T Enqvist [13], A Ereditato [14], F von Feilitzsch [15], P Fileviez Perez [16], M Göger-Neff [17], S Gninenko [4], W Gruber [3], C Hagner [12], M Hess [14], K A Hochmuth [17], J Kisiel [18], L Knecht [3], I Kreslo [14], V A Kudryavtsev [19], P Kuusiniemi [13], T Lachenmaier [15], M Laffranchi [3], B Lefievre [10], P K Lightfoot [19], M Lindner [20], J Maalampi [2], M Maltoni [21], A Marchionni [3], T Marrodán Undagoitia [15], J Marteau [1], A Meregaglia [3], M Messina [14], M Mezzetto [22], A Mirizzi [17,23], L Mosca [9], U Moser [14], A Müller [3], G Natterer [3], L Oberauer [15], P Otiougova [3], T Patzak [10], J Peltoniemi [13], W Potzel [15], C Pistillo [14], G G Raffelt [17], E Rondio [24], M Roos [25], B Rossi [14], A Rubbia [3], N Savvinov [14], T Schwetz [26], J Sobczyk [27], N J C Spooner [19], D Stefan [28], A Tonazzo [10], W Trzaska [2], J Ulbricht [3], C Volpe [29], J Winter [15], M Wurm [15], A Zalewska [28] and R Zimmermann [12]

[1] IPNL, Université Claude Bernard Lyon 1, CNRS/IN2P3, 69622 Villeurbanne, France
[2] Department of Physics, University of Jyväskylä, Finland
[3] Institut für Teilchenphysik, ETHZ, Zürich, Switzerland
[4] Institute for Nuclear Research, Russian Academy of Sciences, Moscow, Russia
[5] CEA - Saclay, Gif sur Yvette and APC Paris, France
[6] Dpto Fisica Teorica y del Cosmos & C.A.F.P.E., Universidad de Granada, Spain
[7] Centre de Physique des Particules de Marseille (CPPM), IN2P3-CNRS et Université d'Aix-Marseille II, Marseille, France
[8] LAL, Université Paris-Sud, IN2P3/CNRS, Orsay, France
[9] CEA - Saclay, Gif sur Yvette, France
[10] Astroparticule et Cosmologie (APC), CNRS, Université Paris VII, CEA, Observatoire de Paris, Paris, France
[11] Laboratoire de Physique Nucléaire et des Hautes Energies (LPNHE), IN2P3-CNRS et Universités Paris VI et Paris VII, Paris, France
[12] Universität Hamburg, Institut für Experimentalphysik, Hamburg, Germany
[13] CUPP, University of Oulu, Finland
[14] Laboratorium für Hochenergie Physik, Bern Universität, Bern, Switzerland
[15] Technische Universität München, Physik-Department E15, Garching, Germany
[16] Centro de Fisica Teorica de Particulas, Instituto Superior Tecnico, Departamento de Fisica, Lisboa, Portugal
[17] Max-Planck-Institut für Physik (Werner-Heisenberg-Institut), München, Germany

[18] Institute of Physics, University of Silesia, Katowice, Poland
[19] Department of Physics and Astronomy, University of Sheffield, Sheffield, United Kingdom
[20] Max-Planck-Institut fuer Kernphysik, Heidelberg, Germany
[21] Departamento de Física Teórica & Instituto de Física Teórica, Facultad de Ciencias C-XI, Universidad Autónoma de Madrid, Cantoblanco, Madrid, Spain
[22] INFN Sezione di Padova, Padova, Italy
[23] INFN Sezione di Bari and Dipartimento di Fisica, Università di Bari, Bari, Italy
[24] A. Soltan Institute for Nuclear Studies, Warsaw, Poland
[25] Department of Physical Sciences, University of Helsinki, Finland
[26] CERN, Physics Department, Theory Division, Geneva, Switzerland
[27] Institute of Theoretical Physics, Wroclaw University, Wroclaw, Poland
[28] H. Niewodniczanski Institute of Nuclear Physics, Krakow, Poland
[29] Institut de Physique Nucleaire d'Orsay (IPNO), Groupe de Physique Theorique, Université de Paris-Sud XI, Orsay, France

E-mail: campagne@lal.in2p3.fr

Abstract.
This document reports on a series of experimental and theoretical studies conducted to assess the astro-particle physics potential of three future large-scale particle detectors proposed in Europe as next generation underground observatories. The proposed apparatus employ three different and, to some extent, complementary detection techniques: GLACIER (liquid Argon TPC), LENA (liquid scintillator) and MEMPHYS (water Cherenkov), based on the use of large mass of liquids as active detection media. The results of these studies are presented along with a critical discussion of the performance attainable by the three proposed approaches coupled to existing or planned underground laboratories, in relation to open and outstanding physics issues such as the search for matter instability, the detection of astrophysical- and geo-neutrinos and to the possible use of these detectors in future high-intensity neutrino beams.

Keywords : neutrino detectors, neutrino experiments, neutrino properties, solar and atmospheric neutrinos, supernova neutrinos, proton decay, wimp

PACS numbers: 13.30.a,14.20.Dh,14.60.Pq,26.65.t+,29.40.Gx,29.40.Ka,29.40.Mc,95.55.Vj,95.85.Ry, 97.60.Bw

Submitted to: *Journal of Cosmology and Astroparticle Physics*

1. Physics motivation

Several outstanding physics goals could be achieved by the next generation of large underground observatories in the domain of astro-particle and particle physics, neutrino astronomy and cosmology. Proton decay [1], in particular, is one of the most exciting prediction of Grand Unified Theories (for a review see [2]) aiming at the unification of fundamental forces in Nature. It remains today one of the most relevant open questions of particle physics. Its discovery would certainly represent a fundamental milestone, contributing to clarifying our understanding of the past and future evolution of the Universe.

Several experiments have been built and conducted to search for proton decay but they only yielded lower limits to the proton lifetime. The window between the predicted proton lifetime (in the simplest models typically below 10^{37} years) and that excluded by experiments [3] ($O(10^{33})$ years, depending on the channel) is within reach, and the demand to fill the gap grows with the progress in other domains of particle physics, astro-particle physics and cosmology. To some extent, also a negative result from next generation high-sensitivity experiments would be relevant to rule-out some of the theoretical models based on SU(5) and SO(10) gauge symmetry or to further constrain the range of allowed parameters. Identifying unambiguously proton decay and measuring its lifetime would set a firm scale for any Unified Theory, narrowing the phase space for possible models and their parameters. This will be a mandatory step to go forward beyond the Standard Model of elementary particles and interactions.

Another important physics subject is the physics of astrophysical neutrinos, as those from supernovae, from the Sun and from the interaction of primary cosmic-rays with the Earth's atmosphere. Neutrinos are above all important messengers from stars. Neutrino astronomy has a glorious although recent history, from the detection of solar neutrinos [4, 5, 6, 7, 8, 9, 10] to the observation of neutrinos from supernova explosion, [11, 12, 13], acknowledged by the Nobel Prizes awarded to M. Koshiba and R. Davis. These observations have given valuable information for a better understanding of the functioning of stars and of the properties of neutrinos. However, much more information could be obtained if the energy spectra of stellar neutrinos were known with higher accuracy. Specific neutrino observations could give detailed information on the conditions of the production zone, whether in the Sun or in a supernova. A supernova explosion in our galaxy would be extremely important as the evolution mechanism of the collapsed star is still a puzzle for astrophysics. An even more fascinating challenge would be observing neutrinos from extragalactic supernovae, either from identified sources or from a diffuse flux due to unidentified past supernova explosions.

Observing neutrinos produced in the atmosphere as cosmic-ray secondaries [14, 15, 16, 17, 18, 19, 20] gave the first compelling evidence for neutrino oscillation [21, 22], a process that unambiguously points to the existence of new physics. While today the puzzle of missing atmospheric neutrinos can be considered solved, there remain challenges related to the sub-dominant oscillation phenomena. In particular, precise measurements of atmospheric neutrinos with high statistics and small systematic errors [23] would help in resolving ambiguities and degeneracies that hamper the interpretation of other experiments, as those planned for future long baseline neutrino oscillation measurements.

Another example of outstanding open questions is that of the knowledge of the interior of the Earth. It may look hard to believe, but we know much better what

happens inside the Sun than inside our own planet. There are very few messengers that can provide information, while a mere theory is not sufficient for building a credible model for the Earth. However, there is a new unexploited window to the Earth's interior, by observing neutrinos produced in the radioactive decays of heavy elements in the matter. Until now, only the KamLAND experiment [24] has been able to study these so-called geo-neutrinos opening the way to a completely new field of research. The small event rate, however, does not allow to draw significant conclusions.

The fascinating physics phenomena outlined above, in addition to other important subjects that we will address in the following, could be investigated by a new generation of multipurpose experiments based on improved detection techniques. The envisioned detectors must necessarily be very massive (and consequently large) due to the smallness of the cross-sections and to the low rate of signal events, and able to provide very low experimental background. The required signal to noise ratio can only be achieved in underground laboratories suitably shielded against cosmic-rays and environmental radioactivity. We can identify three different and, to large extent, complementary technologies capable to meet the challenge, based on large scale use of liquids for building large-size, volume-instrumented detectors

- Water Cherenkov. As the cheapest available (active) target material, water is the only liquid that is realistic for extremely large detectors, up to several hundreds or thousands of ktons; water Cherenkov detectors have sufficiently good resolution in energy, position and angle. The technology is well proven, as previously used for the IMB, Kamiokande and Super-Kamiokande experiments.
- Liquid scintillator. Experiments using a liquid scintillator as active target provide high-energy resolution and offer low-energy threshold. They are particularly attractive for low energy particle detection, as for example solar neutrinos and geo-neutrinos. Also liquid scintillator detectors feature a well established technology, already successfully applied at relatively large scale to the Borexino [25] and KamLAND [26] experiments.
- Liquid Argon Time Projection Chambers (LAr TPC). This detection technology has among the three the best performance in identifying the topology of interactions and decays of particles, thanks to the bubble-chamber-like imaging performance. Liquid Argon TPCs are very versatile and work well with a wide particle energy range. Experience on such detectors has been gained within the ICARUS project [27, 28].

Three experiments are proposed to employ the above detection techniques: MEMPHYS [29] for water Cherenkov, LENA [30, 31] for liquid scintillator and GLACIER [32, 33, 34, 35, 36] for Liquid Argon. In this paper we report on the study of the physics potential of the experiments and identify features of complementarity amongst the three techniques.

Needless to say, the availability of future neutrino beams from particle accelerators would provide an additional bonus to the above experiments. Measuring oscillations with artificial neutrinos (of well known kinematical features) with a sufficiently long baseline would allow to accurately determine the oscillation parameters (in particular the mixing angle θ_{13} and the possible CP violating phase in the mixing matrix). The envisaged detectors may then be used for observing neutrinos from the future Beta Beams and Super Beams in the optimal energy range for each experiment. A common example is a low-energy Beta Beam from CERN to MEMPHYS at Frejus, 130 km

Table 1. Basic parameters of the three detector (baseline) design.

	GLACIER	LENA	MEMPHYS
Detector dimensions			
type of cylinder	1 vert.	1 horiz.	$3 \div 5$ vert.
diam. (m)	70	30	65
length (m)	20	100	65
typical mass (kton)	100	50	$600 \div 800$
Active target and readout			
type of target	liq. Argon (boiling)	liq. scintillator	water (opt. 0.2% $GdCl_3$)
readout type	e^- drift: 2 perp. views, 10^5 channels, ampli. in gas phase; Cher. light: 27 000 8" PMTs, $\sim$ 20% coverage; Scint. light: 1000 8" PMTs	12 000 20" PMTs $\gtrsim 30\%$ coverage	81 000 12" PMTs $\sim 30\%$ coverage

away [37]. High energy beams have been suggested [38], favoring longer baselines of up to $O(2000$ km). The ultimate Neutrino Factory facility will require a magnetized detector to fully exploit the simultaneous availability of neutrinos and antineutrinos. This subject is however beyond the scope of the present study.

Finally, there is a possibility of (and the hope for) unexpected discoveries. The history of physics has shown that several experiments have made their glory with discoveries in research fields that were outside the original goals of the experiments. Just to quote an example, we can mention the Kamiokande detector, mainly designed to search for proton decay and actually contributing to the observation of atmospheric neutrino oscillations, to the clarification of the solar neutrino puzzle and to the first observation of supernova neutrinos [11, 39, 5, 15, 21]. All the three proposed experiments, thanks to their outstanding boost in mass and performance, will certainly provide a significant potential for surprises and unexpected discoveries.

2. Description of the three detectors

The three detectors' basic parameters are listed in Tab. 1. All of them have active targets of tens to hundreds kton mass and are to be installed in underground laboratories to be protected against background induced by cosmic-rays. As already said, the large size of the detectors is motivated by the extremely low cross-section of neutrinos and/or by the rareness of the interesting events searched for. Some details of the detectors are discussed in the following, while the matters related to the possible underground site are presented in Section 3.

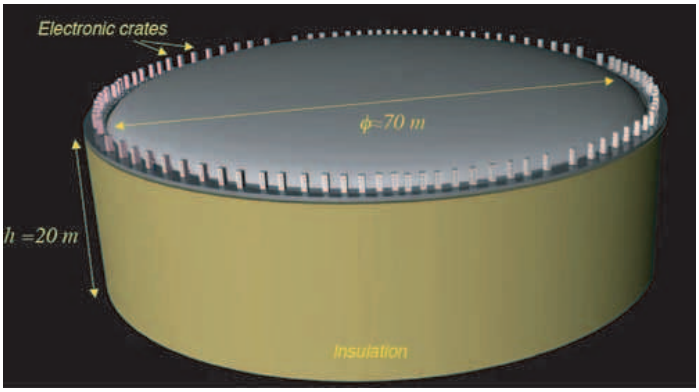

Figure 1. Artistic view of a 100 kton single-tank liquid Argon TPC detector. The electronic crates are located at the top of the dewar.

2.1. Liquid Argon TPC

GLACIER (Fig. 1) is the foreseen extrapolation up to 100 kton of the liquid Argon Time Projection Chamber technique. The detector can be mechanically subdivided into two parts, the liquid Argon tank and the inner detector instrumentation. For simplicity, we assume at this stage that the two aspects can be largely decoupled.

The basic idea behind this detector is to use a single 100 kton boiling liquid Argon cryogenic tank with cooling directly performed with liquid Argon (self-refrigerating). Events are reconstructed in 3D by using the information provided by ionization in liquid. The imaging capabilities and the excellent space resolution of the device make this detector an "electronic bubble chamber". The signal from scintillation and Cherenkov light readout complete the information contributing to the event reconstruction.

As far as light collection is concerned one can profit from the ICARUS R&D program that has shown that it is possible to operate photomultipliers (PMTs) directly immersed in the liquid Argon [27]. In order to be sensitive to deep UV (DUV) scintillation ($<$ 300nm), PMTs are coated with a wavelength shifter (WLS), for instance tetraphenyl-butadiene. About 1000 immersed phototubes with WLS would be used to identify the (isotropic and bright) scintillation light. To detect Cherenkov radiation about 27 000 8"-phototubes without WLS would provide a 20% coverage of the detector surface. The latter PMTs should have single photon counting capabilities in order to count the number of Cherenkov photons.

Charge amplification and an extreme liquid purity against electronegative compounds (although attainable by commercial purification systems) is needed to allow long drift distances of the ionization/imaging electrons ($\approx$ 20 m). For this reason, the detector will run in the so-called bi-phase mode. Namely, drifting electrons produced in the liquid phase are extracted into the gas phase with the help of an electric field and amplified in order to compensate the charge loss due to attenuation along the drift path. The final charge signal is then read out by means of Large Electron Multiplier (LEM) devices, providing X-Y information. The Z coordinate is given by the drift time measurement, proportional to the drift length. A possible extension of the present detector design envisages the immersion of the sensitive

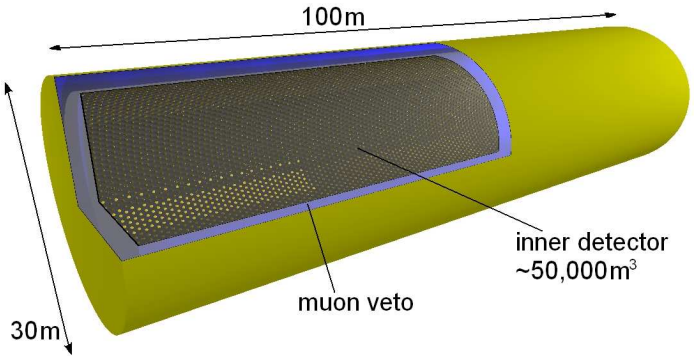

Figure 2. Schematic drawing of the LENA detector. Reprinted figure with the permission from [40].

volume in an external magnetic field [36]. Existing experience from specialized Liquified Natural Gases (LNG) companies and studies conducted in collaboration with Technodyne LtD UK, have been ingredients for a first step in assessing the feasibility of the detector and of its operation in an underground site.

2.2. Liquid scintillator detector

The LENA detector is cylindrical in shape with a length of about 100 m and 30 m diameter (Fig. 2). The inner volume corresponding to a radius of 13 m contains approximately 5×10^4 m^3 of liquid scintillator. The outer part of the volume is filled with water, acting as a veto for identifying muons entering the detector from outside. Both the outer and the inner volume are enclosed in steel tanks of 3 to 4 cm wall thickness. For most purposes, a fiducial volume is defined by excluding the volume corresponding to 1 m distance to the inner tank walls. The fiducial volume so defined amounts to 88 % of the total detector volume.

In the current design, the main axis of the cylinder is placed horizontally. A tunnel-shaped cavern housing the detector is considered as realistically feasible for most of the envisioned detector locations. In respect to accelerator physics, the axis could be oriented towards the neutrino source in order to contain the full length of muon and electron tracks produced in charged-current neutrino interactions in the liquid scintillator.

The baseline configuration for the light detection in the inner volume foresees 12 000 PMTs of 20" diameter mounted onto the inner cylinder wall and covering about 30 % of the surface. As an option, light concentrators can be installed in front of the PMTs, hence increasing the surface coverage c to values larger than 50 %. Alternatively, $c = 30$ % can be reached by equipping 8" PMTs with light concentrators, thereby reducing the cost when comparing to the baseline configuration. Additional PMTs are supplied in the outer veto to detect (and reject) the Cherenkov light from events due to incoming cosmic muons. Possible candidates as liquid scintillator material are pure phenyl-o-xylylethane (PXE), a mixture of 20 % PXE and 80 % Dodecane, and linear Alkylbenzene (LAB). All three liquids exhibit low toxicity and provide high flash and inflammation points.

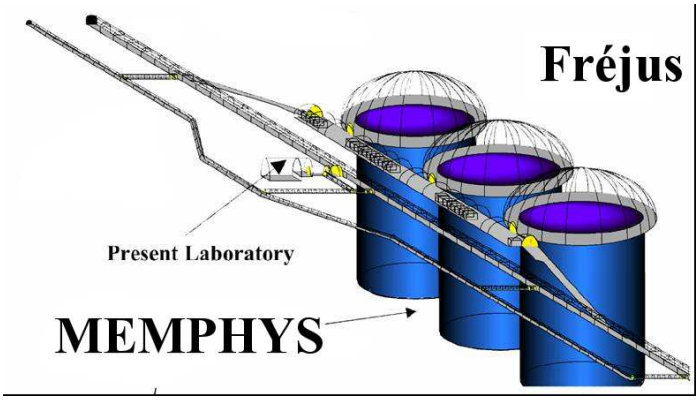

Figure 3. Layout of the MEMPHYS detector in the future Fréjus laboratory.

2.3. Water Cherenkov

The MEMPHYS detector (Fig. 3) is an extrapolation of the water Cherenkov Super-Kamiokande detector to a mass as large as 730 kton. The detector is composed of up to 5 shafts containing separate tanks. 3 tanks are enough to total 440 kton fiducial mass. This is the configuration which is used hereafter. Each shaft has 65 m diameter and 65 m height representing an increase by a factor 8 with respect to Super-Kamiokande.

The Cherenkov light rings produced by fast particles moving within the inner water volume are reconstructed by PMTs placed on the inner tank wall. The PMT housing surface starts at 2 m from the outer wall and is covered with about 81 000 12" PMTs to reach a 30% surface coverage, in or alternatively equivalent to a 40% coverage with 20" PMTs. The fiducial volume is defined by an additional conservative guard of 2 m. The outer volume between the PMT surface and the water vessel is instrumented with 8" PMTs. If not otherwise stated, the Super-Kamiokande analysis procedures for efficiency calculations, background reduction, etc. are used in computing the physics potential of MEMPHYS. In USA and Japan, two analogous projects (UNO and Hyper-Kamiokande) have been proposed. These detectors are similar in many respects and the physics potential presented hereafter may well be transposed to them. Specific characteristics that are not identical in the proposed projects are the distance from available or envisaged accelerators and nuclear reactors, sources of artificial neutrino fluxes, and the depth of the host laboratory.

Currently, there is a very promising ongoing R&D activity concerning the possibility of introducing Gadolinium salt ($GdCl_3$) inside Super-Kamiokande. The physics goal is to decrease the background for many physics channels by detecting and tagging neutrons produced in the Inverse Beta Decay (IBD) interaction of $\bar{\nu}_e$ on free protons. For instance, 100 tons of $GdCl_3$ in Super-Kamiokande would yield more then 90% neutron captures on Gd [41].

3. Underground sites

The proposed large detectors require underground laboratories of adequate size and depth, naturally protected against cosmic-rays that represent a potential source of background events mainly for non-accelerator experiments, that cannot exploit the

peculiar time stamp provided by the accelerator beam spill.

Additional characteristics of these sites contributing to their qualification as candidates for the proposed experiments are: the type and quality of the rock allowing the practical feasibility of large caverns at reasonable cost and within reasonable time, the distance from existing (or future) accelerators and nuclear reactors, the type and quality of the access, the geographical position, the environmental conditions, etc.

The presently identified worldwide candidate sites are located in three geographical regions: North-America, far-east Asia and Europe. In this paper we consider the European region, where, at this stage, the following sites are assumed as candidates: Boulby (UK), Canfranc (Spain), Fréjus (France/Italy), Gran Sasso (Italy), Pyhäsalmi (Finland) and Sieroszewice (Poland). Most of the sites are existing national or international underground laboratories with associated infrastructure and experimental halls already used for experiments. The basic features of the sites are presented on Tab. 2. For the Gran Sasso Laboratory a possible new (additional) site is envisaged to be located 10 km away from the present underground laboratory, outside the protected area of the neighboring Gran Sasso National Park. The possibility of under-water solutions, such as for instance Pylos for the LENA project, is not taken into account here. The identification and measurement of the different background components in the candidate sites (muons, fast neutrons from muon interactions, slow neutrons from nuclear reactions in the rock, gammas, electrons/positrons and alphas from radioactive decays,...) is underway, mainly in the context of the ILIAS European (JRA) Network ($http://ilias.in2p3.fr/$).

None of the existing sites has yet a sufficiently large cavity able to accommodate the foreseen detectors. For two of the sites (Fréjus and Pyhäsalmi) a preliminary feasibility study for large excavation at deep depth has already been performed. For the Fréjus site the main conclusion drawn from simulations constrained by a series of rock parameter measurements made during the Fréjus road tunnel excavation is that the "shaft shape" is strongly preferred compared to the "tunnel shape", as long as large cavities are required. As mentioned above, several (up to 5) of such shaft cavities with a diameter of about 65 m (for a corresponding volume of 250 000 m^3) each, seem feasible in the region around the middle of the Fréjus tunnel, at a depth of 4800 m.w.e. For the Pyhäsalmi site, the preliminary study has been performed for two main cavities with tunnel shape and dimensions of $(20 \times 20 \times 120)$ m^3 and $(20 \times 20 \times 50)$ m^3, respectively, and for one shaft-shaped cavity with 25 m in diameter and 25 m in height, all at a depth of about 1430 m of rock (4000 m.w.e.).

4. Matter instability: sensitivity to proton decay

For all relevant aspects of the proton stability in Grand Unified Theories, in strings and in branes we refer to [2]. Since proton decay is the most dramatic prediction coming from theories of the unification of fundamental interactions, there is a realistic hope to be able to test these scenarios with next generation experiments exploiting the above mentioned large mass, underground detectors. For this reason, the knowledge of a theoretical upper bound on the lifetime of the proton is very helpful in assessing the potential of future experiments. Recently, a model-independent upper bound on the proton decay lifetime has been worked out [42]

$$\tau_p^{upper} = \left\{ \begin{array}{ll} 6.0 \times 10^{39} & \text{(Majorana)} \\ 2.8 \times 10^{37} & \text{(Dirac)} \end{array} \right\} \times \frac{\left(M_X/10^{16} GeV\right)^4}{\alpha_{GUT}^2} \times \left(\frac{0.003 GeV^3}{\alpha}\right)^2 \text{ years} \quad (1)$$

Table 2. Summary of characteristics of some underground sites envisioned for the proposed detectors.

Site	Boulby	Canfranc	Fréjus	Gran Sasso	Pyhäsalmi	Sieroszowice
Location	UK	Spain	Italy-France border	Italy	Finland	Poland
Dist. from CERN (km)	1050	630	130	730	2300	950
Type of access	Mine	Somport tunnel	Fréjus tunnel	Highway		
tunnel	Mine	Shaft				
Vert. depth (m.w.e)	2800	2450	4800	3700	4000	2200
Type of rock	salt	hard rock	hard rock	hard rock	hard rock	salt & rock
Type of cavity			shafts		tunnel	shafts
Size of cavity			$\Phi = 65$ m		$(20 \times 20 \times 120)\mathrm{m}^3$	$\Phi = 74$ m
			$H = 80$ m			$H = 37$ m
μ Flux ($\mathrm{m}^{-2}\mathrm{day}^{-1}$)	34	406	4	24	9	not available

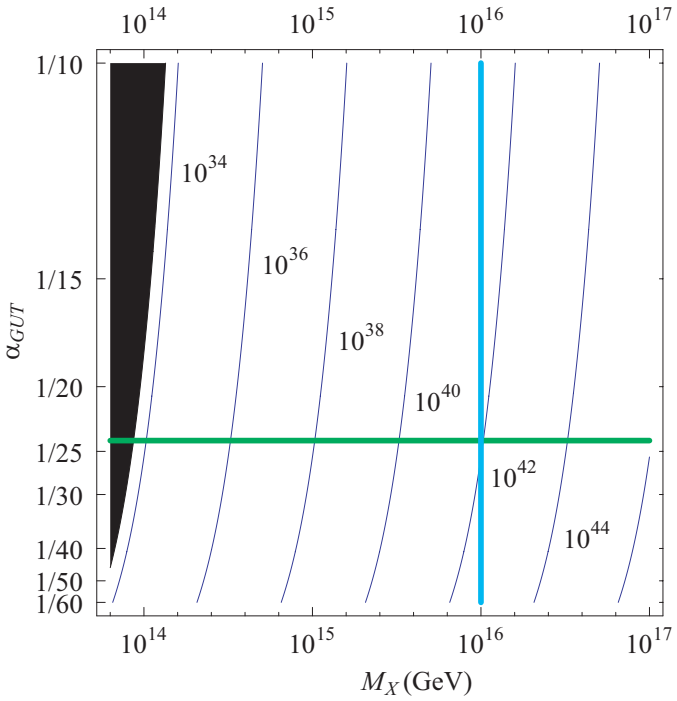

Figure 4. Isoplot for the upper bounds on the total proton lifetime in years in the Majorana neutrino case in the M_X–α_{GUT} plane. The value of the unifying coupling constant is varied from 1/60 to 1/10. The conventional values for M_X and α_{GUT} in SUSY GUTs are marked with thick lines. The experimentally excluded region is given in black. Reprinted figure with permission from [42].

where M_X is the mass of the superheavy gauge bosons mediating proton decay, the parameter $\alpha_{GUT} = g^2_{GUT}/4\pi$, with g_{GUT} the gauge coupling at the grand unified scale and α is the relevant matrix element. Fig. 4 shows the present parameter space allowed by experiments in the case of Majorana neutrinos.

Most of the models (Super-symmetric or non Super-symmetric) predict a proton lifetime τ_p below those upper bounds (10^{33-37} years). This is particularly interesting since this falls within the possible range of the proposed experiments. In order to have a better idea of the proton decay predictions, we list the results from different models in Tab. 3.

No specific simulations for MEMPHYS have been carried out yet. Therefore, here we rely on the studies done for the similar UNO detector, adapting the results to MEMPHYS, which, however, features an overall better PMT coverage.

In order to assess the physics potential of a large liquid Argon Time Projection Chambers such as GLACIER, a detailed simulation of signal efficiency and background sources, including atmospheric neutrinos and cosmogenic backgrounds was carried out [58]. Liquid Argon TPCs, offering high space granularity and energy resolution, low-energy detection threshold, and excellent background discrimination, should yield large signal over background ratio for many of the possible proton decay modes, hence allowing reaching partial lifetime sensitivities in the range of $10^{34} - 10^{35}$ years for

Table 3. Summary of several predictions for the proton partial lifetimes (years). References for the different models are: (1) [43], (2) [44, 45], (3) [46], (4) [47, 48, 49, 50], (5) [51, 52, 53, 54], (6) [55], (7) [56], (8) [57].

Model	Decay modes	Prediction	References
Georgi-Glashow model	-	ruled out	(1)
Minimal realistic non-SUSY $SU(5)$	all channels	$\tau_p^{upper} = 1.4 \times 10^{36}$	(2)
Two Step Non-SUSY $SO(10)$	$p \to e^+\pi^0$	$\approx 10^{33-38}$	(3)
Minimal SUSY $SU(5)$	$p \to \bar{\nu}K^+$	$\approx 10^{32-34}$	(4)
SUSY $SO(10)$ with 10_H, and 126_H	$p \to \bar{\nu}K^+$	$\approx 10^{33-36}$	(5)
M-Theory(G_2)	$p \to e^+\pi^0$	$\approx 10^{33-37}$	(6)
$SU(5)$ with 24_F	$p \to \pi^0 e^+$	$\approx 10^{35-36}$	(7)
Renormalizable Adjoint $SU(5)$	$p \to \pi^0 e^+$	$\approx 10^{35-36}$	(8)

exposures up to 1000 kton year. This can often be accomplished in quasi background-free conditions optimal for discoveries at the few events level, corresponding to atmospheric neutrino background rejections of the order of 10^5.

Multi-prong decay modes like $p \to \mu^-\pi^+K^+$ or $p \to e^+\pi^+\pi^-$ and channels involving kaons like $p \to K^+\bar{\nu}$, $p \to e^+K^0$ and $p \to \mu^+K^0$ are particularly appealing, since liquid Argon imaging provides typically one order of magnitude efficiency increase for similar or better background conditions, compared to water Cherenkov detectors. Thanks to the clean photon identification and separation from π^0, it is expected an efficiency of 98% for both the channels $p \to e^+\gamma$ and $p \to \mu^+\gamma$ which constitute an improvement of 35% and 92% respectively compared to Super-Kamiokande present result. Channels such as $p \to e^+\pi^0$ and $p \to \mu^+\pi^0$, dominated by intrinsic nuclear effects, yield similar performance as water Cherenkov detectors.

An important feature of GLACIER is that thanks to the self-shielding and 3D-imaging properties, the above expected performance remains valid even at shallow depths, where cosmogenic background sources are important. The possibility of using a very large-area, annular, muon-veto active shielding, to further suppress cosmogenic backgrounds at shallow depths is also a very promising option to complement the GLACIER detector.

In order to quantitatively estimate the potential of the LENA detector in measuring proton lifetime, a Monte Carlo simulation for the decay channel $p \to K^+\overline{\nu}$ has been performed. For this purpose, the GEANT4 simulation toolkit [59] has been used, including optical processes as scintillation, Cherenkov light production, Rayleigh scattering and light absorption. From these simulations one obtains a light yield of $\sim$ 110 p.e./MeV [60] for an event in the center of the detector. In addition, the semi-empirical Birk's formula has been introduced into the code in order to take into account the so-called quenching effects.

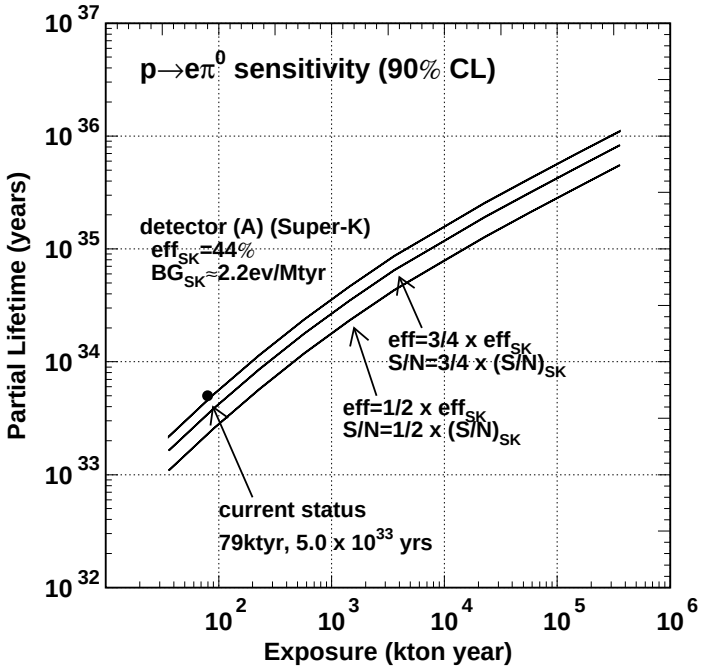

Figure 5. Sensitivity to the $e^+\pi^0$ proton decay mode compiled by the UNO collaboration. MEMPHYS corresponds to case (A). Reprinted figure with permission from [61].

Following studies performed for the UNO detector, the detection efficiency for $p \to e^+\pi^0$ is 43% for a 20" PMT coverage of 40% or its equivalent, as envisioned for MEMPHYS. The corresponding estimated atmospheric neutrino induced background is at the level of 2.25 events/Mton year. From these efficiencies and background levels, proton decay sensitivity as a function of detector exposure can be estimated. A 10^{35} years partial lifetime (τ_p/B) could be reached at the 90% C.L. for a 5 Mton year exposure (10 years) with MEMPHYS (similar to case A in Fig. 5 compiled by the UNO collaboration [61]). Beyond that exposure, tighter cuts may be envisaged to further reduce the atmospheric neutrino background to 0.15 events/Mton year, by selecting quasi exclusively the free proton decays.

The positron and the two photons issued from the π^0 gives clear events in the GLACIER detector. The π^0 is absorbed by the nucleus in 45% of the cases. Assuming a perfect particle and track identification, one may expect a 45% efficiency and a background level of 1 event/Mton year. For a 1 Mton year (10 years) exposure with GLACIER one reaches $\tau_p/B > 0.4 \times 10^{35}$ years at the 90% C.L. (Fig. 6).

In a liquid scintillator detector such as LENA the decay $p \to e^+\pi^0$ would produce a 938 MeV signal coming from the e^+ and the π^0 shower. Only atmospheric neutrinos are expected to cause background events in this energy range. Using the fact that showers from both e^+ and π^0 propagate 4 m in opposite directions before being stopped, atmospheric neutrino background can be reduced. Applying this method, the current limit for this channel ($\tau_p/B = 5.4\ 10^{33}$ years [62]) could be improved. In LENA, proton decay events via the mode $p \to K^+\overline{\nu}$ have a very clear signature.

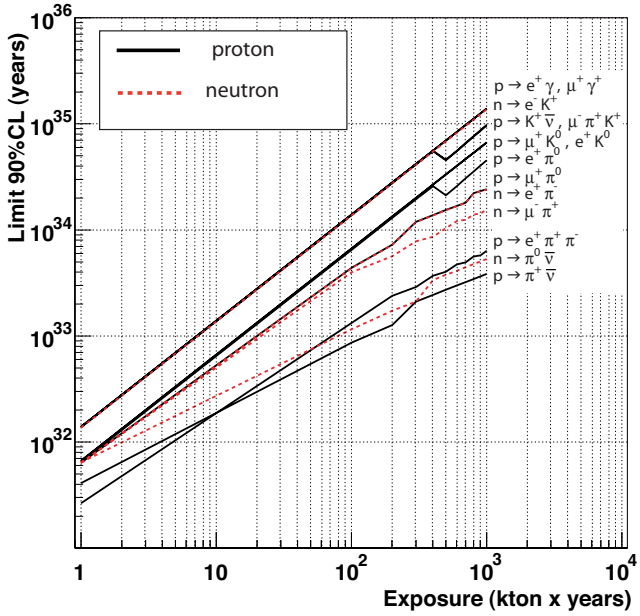

Figure 6. Expected proton decay lifetime limits (τ/B at 90% C.L.) as a function of exposure for GLACIER. Only atmospheric neutrino background has been taken into account. Reprinted figure with permission from [58].

The kaon causes a prompt monoenergetic signal of 105 MeV together with a larger delayed signal from its decay. The kaon has a lifetime of 12.8 ns and two main decay channels: with a probability of 63.43 % it decays via $K^+ \rightarrow \mu^+\nu_\mu$ and with 21.13%, via $K^+ \rightarrow \pi^+\pi^0$.

Simulations of proton decay events and atmospheric neutrino background have been performed and a pulse shape analysis has been applied. From this analysis an efficiency of 65% for the detection of a proton decay has been determined and a background suppression of $\sim 2 \times 10^4$ has been achieved [60]. A detail study of background implying pion and kaon production in atmospheric neutrino reactions has been performed leading to a background rate of 0.064 year^{-1} due to the reaction $\nu_\mu + p \rightarrow \mu^- + K^+ + p$.

For the current proton lifetime limit for the channel considered ($\tau_p/B = 2.3 \times 10^{33}$ year) [3], about 40.7 proton decay events would be observed in LENA after ten years with less than 1 background event. If no signal is seen in the detector within ten years, the lower limit for the lifetime of the proton will be set at $\tau_p/B > 4 \times 10^{34}$ years at the 90% C.L.

For GLACIER, the latter is a quite clean channel due to the presence of a strange meson and no other particles in the final state. Using dE/dx versus range as the discriminating variable in a Neural Network algorithm, less than 1% of the kaons are mis-identified as protons. For this channel, the selection efficiency is high (97%) for an atmospheric neutrino background < 1 event/Mton year. In case of absence of signal and for a detector location at a depth of 1 km.w.e., one expects for 1 Mton year

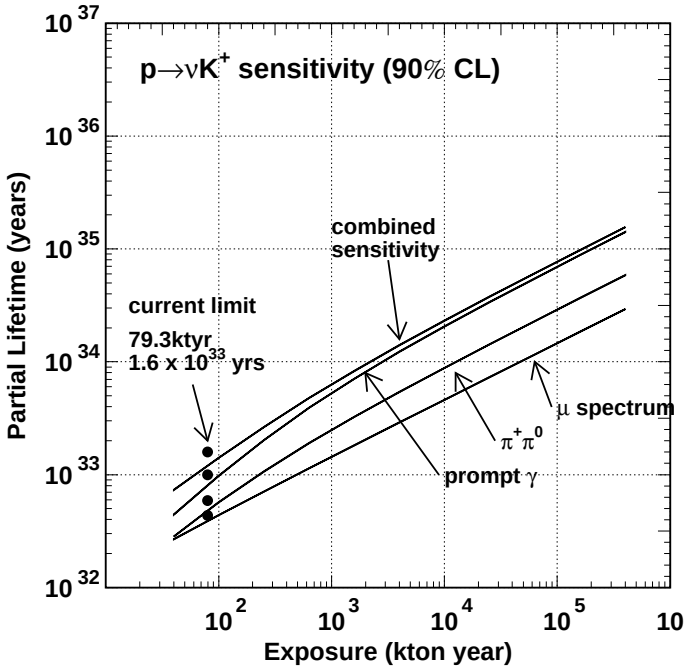

Figure 7. Expected sensitivity to the νK^+ proton decay mode as a function of exposure compiled by the UNO collaboration which may be applied for the MEMPHYS detector (see text for details). Reprinted figure with permission from [61].

(10 years) exposure one background event due to cosmogenic sources. This translates into a limit $\tau_p/B > 0.6 \times 10^{35}$ years at 90% C.L. This result remains valid even at shallow depths where cosmogenic background sources are a very important limiting factor for proton decay searches. For example, the study done in [58] shows that a three-plane active veto at a shallow depth of about 200 m rock overburden under a hill yields similar sensitivity for $p \to K^+\bar{\nu}$ as a 3000 m.w.e. deep detector.

For MEMPHYS one should rely on the detection of the decay products of the K^+ since its momentum (340 MeV/c) is below the water Cherenkov threshold of 570 MeV/c: a 236 MeV/c muon and its decay electron (type I) or a 205 MeV/c π^+ and π^0 (type II), with the possibility of a delayed (12 ns) coincidence with the 6 MeV ^{15}N de-excitation prompt γ (Type III). Using the known imaging and timing performance of Super-Kamiokande, the efficiency for the reconstruction of $p \to \overline{\nu}K^+$ is 33% (I), 6.8% (II) and 8.8% (III), and the background is 2100, 22 and 6 events/Mton year, respectively. For the prompt γ method, the background is dominated by miss-reconstruction. As stated by the UNO Collaboration [61], there are good reasons to believe that this background can be lowered by at least a factor of two, corresponding to the atmospheric neutrino interaction $\nu p \to \nu \Lambda K^+$. In these conditions, and taking into account the Super-Kamiokande performance, a 5 Mton year exposure for MEMPHYS would allow reaching $\tau_p/B > 2 \times 10^{34}$ years (Fig. 7).

A preliminary comparison between the performance of three detectors has been carried out (Tab. 4). For the $e^+\pi^0$ channel, the Cherenkov detector gets a better

Table 4. Summary of the $e^+\pi^0$ and $\bar{\nu}K^+$ decay discovery potential for the three detectors. The $e^+\pi^0$ channel is not yet simulated for LENA.

	GLACIER	LENA	MEMPHYS
$e^+\pi^0$			
ϵ(%)/Bkgd(Mton year)	45/1	-	43/2.25
τ_p/B (90% C.L., 10 years)	0.4×10^{35}	-	1.0×10^{35}
$\bar{\nu}K^+$			
ϵ(%)/Bkgd(Mton year)	97/1	65/1	8.8/3
τ_p/B (90% C.L., 10 years)	0.6×10^{35}	0.4×10^{35}	0.2×10^{35}

limit due to the higher mass. However, it should be noted that GLACIER, although five times smaller in mass than MEMPHYS, can reach a limit that is only a factor two smaller. Liquid Argon TPCs and liquid scintillator detectors obtain better results for the $\bar{\nu}K^+$ channel, due to their higher detection efficiency. The techniques look therefore quite complementary. We have also seen that GLACIER does not necessarily requires very deep underground laboratories, like those currently existing or future planned sites, in order to perform high sensitivity nucleon decay searches.

5. Supernova neutrinos

The detection of supernova (SN) neutrinos represents one of the next frontiers of neutrino physics and astrophysics. It will provide invaluable information on the astrophysics of the core-collapse explosion phenomenon and on the neutrino mixing parameters. In particular, neutrino flavor transitions in the SN envelope might be sensitive to the value of θ_{13} and to the type of mass hierarchy. These two main issues are discussed in detail in the following Sections.

5.1. SN neutrino emission, oscillation and detection

A core-collapse supernova marks the evolutionary end of a massive star ($M \gtrsim 8\,M_\odot$) which becomes inevitably unstable at the end of its life. The star collapses and ejects its outer mantle in a shock-wave driven explosion. The collapse to a neutron star ($M \simeq M_\odot$, $R \simeq 10$ km) liberates a gravitational binding energy of $\approx 3 \times 10^{53}$ erg, 99% of which is transferred to (anti) neutrinos of all the flavors and only 1% to the kinetic energy of the explosion. Therefore, a core-collapse SN represents one of the most powerful sources of (anti) neutrinos in the Universe. In general, numerical simulations of SN explosions provide the original neutrino spectra in energy and time F^0_ν. Such initial distributions are in general modified by flavor transitions in the SN envelope, in vacuum (and eventually in Earth matter): $F^0_\nu \longrightarrow F_\nu$ and must be convoluted with the differential interaction cross-section σ_e for electron or positron production, as well as with the detector resolution function R_e and the efficiency ε, in order to finally get observable event rates $N_e = F_\nu \otimes \sigma_e \otimes R_e \otimes \varepsilon$.

Regarding the initial neutrino distributions F^0_ν, a SN collapsing core is roughly a black-body source of thermal neutrinos, emitted on a timescale of ~ 10 s. Energy spectra parametrizations are typically cast in the form of quasi-thermal distributions, with typical average energies: $\langle E_{\nu_e} \rangle = 9 - 12$ MeV, $\langle E_{\bar{\nu}_e} \rangle = 14 - 17$ MeV, $\langle E_{\nu_x} \rangle = 18 - 22$ MeV, where ν_x indicates any non-electron flavor.

Table 5. Values of the p and $\bar{p}$ parameters used in Eq. 2 in different scenario of mass hierarchy and $\sin^2\theta_{13}$.

Mass Hierarchy	$\sin^2\theta_{13}$	p	$\bar{p}$
Normal	$\gtrsim 10^{-3}$	0	$\cos^2\theta_{12}$
Inverted	$\gtrsim 10^{-3}$	$\sin^2\theta_{12}$	0
Any	$\lesssim 10^{-5}$	$\sin^2\theta_{12}$	$\cos^2\theta_{12}$

The oscillated neutrino fluxes arriving on Earth may be written in terms of the energy-dependent survival probability p ($\bar{p}$) for neutrinos (antineutrinos) as [63]

$$\begin{aligned} F_{\nu_e} &= pF^0_{\nu_e} + (1-p)F^0_{\nu_x} \\ F_{\bar{\nu}_e} &= \bar{p}F^0_{\bar{\nu}_e} + (1-\bar{p})F^0_{\nu_x} \\ 4F_{\nu_x} &= (1-p)F^0_{\nu_e} + (1-\bar{p})F^0_{\bar{\nu}_e} + (2+p+\bar{p})F^0_{\nu_x} \end{aligned} \tag{2}$$

where ν_x stands for either ν_μ or ν_τ. The probabilities p and $\bar{p}$ crucially depend on the neutrino mass hierarchy and on the unknown value of the mixing angle θ_{13} as shown in Tab. 5.

Galactic core-collapse supernovae are rare, perhaps a few per century. Up to now, SN neutrinos have been detected only once during the SN 1987A explosion in the Large Magellanic Cloud in 1987 ($d = 50$ kpc). Due to the relatively small masses of the detectors operational at that time, only few events were detected: 11 in Kamiokande [11, 39] and 8 in IMB [64, 12]. The three proposed large-volume neutrino observatories can guarantee continuous exposure for several decades, so that a high-statistics SN neutrino signal could be eventually observed. The expected number of events for GLACIER, LENA and MEMPHYS are reported in Tab. 6 for a typical galactic SN distance of 10 kpc. The total number of events is shown in the upper panel, while the lower part refers to the ν_e signal detected during the prompt neutronization burst, with a duration of ~ 25 ms, just after the core bounce.

The $\bar{\nu}_e$ detection by Inverse Beta Decay (IBD) is the golden channel for MEMPHYS and LENA. In addition, the electron neutrino signal can be detected by LENA thanks to the interaction on ^{12}C. The three charged-current reactions would provide information on ν_e and $\bar{\nu}_e$ fluxes and spectra while the three neutral-current processes, sensitive to all neutrino flavours, would give information on the total flux. GLACIER has also the opportunity to detect ν_e by charged-current interactions on ^{40}Ar with a very low energy threshold. The detection complementarity between ν_e and $\bar{\nu}_e$ is of great interest and would assure a unique way of probing the SN explosion mechanism as well as assessing intrinsic neutrino properties. Moreover, the huge statistics would allow spectral studies in time and in energy domain.

We wish to stress that it will be difficult to establish SN neutrino oscillation effects solely on the basis of a $\bar{\nu}_e$ or ν_e spectral hardening, relative to theoretical expectations. Therefore, in the recent literature the importance of model-independent signatures has been emphasized. Here we focus mainly on signatures associated to the prompt ν_e neutronization burst, the shock-wave propagation and the Earth matter crossing.

The analysis of the time structure of the SN signal during the first few tens of milliseconds after the core bounce can provide a clean indication if the full ν_e burst is present or absent, and therefore allows distinguishing between different mixing

Table 6. Summary of the expected neutrino interaction rates in the different detectors for a typical SN. The following notations have been used: CC, NC, IBD, eES and pES stand for Charged Current, Neutral Current, Inverse Beta Decay, electron and proton Elastic Scattering, respectively. The final state nuclei are generally unstable and decay either radiatively (notation *), or by β^-/β^+ weak interaction (notation $^{-,+}$). The rates of the different reaction channels are listed, and for LENA they have been obtained by scaling the predicted rates from [65, 66].

MEMPHYS		LENA		GLACIER	
Interaction	Rates	Interaction	Rates	Interaction	Rates
$\bar{\nu}_e$ IBD	2×10^5	$\bar{\nu}_e$ IBD	9.0×10^3	$\nu_e^{CC}(^{40}Ar, ^{40}K^*)$	2.5×10^4
$\overset{(-)}{\nu}{}_e^{CC}(^{16}O, X)$	1×10^4	ν_x pES	7.0×10^3	$\nu_x^{NC}(^{40}Ar^*)$	3.0×10^4
ν_x eES	1×10^3	$\nu_x^{NC}(^{12}C^*)$	3.0×10^3	ν_x eES	1.0×10^3
		ν_x eES	6.0×10^2	$\bar{\nu}_e^{CC}(^{40}Ar, ^{40}Cl^*)$	5.4×10^2
		$\bar{\nu}_e^{CC}(^{12}C, ^{12}B^+)$	5.0×10^2		
		$\nu_e^{CC}(^{12}C, ^{12}N^-)$	8.5×10^1		
Neutronization Burst rates					
MEMPHYS	60	ν_e eES			
LENA	70	ν_e eES/pES			
GLACIER	380	$\nu_x^{NC}(^{40}Ar^*)$			

scenarios, as indicated by the third column of Tab. 7. For example, if the mass ordering is normal and θ_{13} is large, the ν_e burst will fully oscillate into ν_x. If θ_{13} turns out to be relatively large one could be able to distinguish between normal and inverted neutrino mass hierarchy.

As discussed above, MEMPHYS is mostly sensitive to the IBD, although the ν_e channel can be measured by the elastic scattering reaction $\nu_x + e^- \to e^- + \nu_x$ [67]. Of course, the identification of the neutronization burst is the cleanest with a detector exploiting the charged-current absorption of ν_e neutrinos, such as GLACIER. Using its unique features of measuring ν_e CC (Charged Current) events it is possible to probe oscillation physics during the early stage of the SN explosion, while with NC (Neutral Current) events one can decouple the SN mechanism from the oscillation physics [68, 69].

A few seconds after core bounce, the SN shock wave will pass the density region in the stellar envelope relevant for oscillation matter effects, causing a transient modification of the survival probability and thus a time-dependent signature in the neutrino signal [70, 71]. This would produce a characteristic dip when the shock wave passes [72], or a double-dip if a reverse shock occurs [73]. The detectability of such a signature has been studied in a large water Cherenkov detector like MEMPHYS by the IBD [72], and in a liquid Argon detector like GLACIER by Argon CC interactions [74]. The shock wave effects would certainly be visible also in a large volume scintillator such as LENA. Such observations would test our theoretical understanding of the core-collapse SN phenomenon, in addition to identifying the actual neutrino mixing scenario.

Nevertheless, the supernova matter profile need not be smooth. Behind the shock-wave, convection and turbulence can cause significant stochastic density fluctuations which tend to cast a shadow by making other features, such as the shock front,

unobservable in the density range covered by the turbulence [75, 76]. The quantitative relevance of this effect remains to be understood.

A unambiguous indication of oscillation effects would be the energy-dependent modulation of the survival probability $p(E)$ caused by Earth matter effects [77]. Under the assumption of a definite mass hierarchy (either normal or inverted), the calculation of neutrino conversion probability in Earth can be reduced to a 2 ν problem, so that Tab. 5 and Eq. 2, one can substitute $\cos^2\theta_{12} \to 1 - P_E$ and $\sin^2\theta_{12} \to P_E$, where $P_E = P(\nu_e \to \nu_2)$ in the Earth. Analytical expression for P_E can be given for particularly simple (or approximated) situations of Earth matter crossing [78, 79]. These effects can be revealed by peculiar wiggles in the energy spectra, due to neutrino oscillations in Earth crossing. In this respect, LENA benefits from a better energy resolution than MEMPHYS, which may be partially compensated by 10 times more statistics [80]. The Earth effect would show up in the $\bar{\nu}_e$ channel for the normal mass hierarchy, assuming that θ_{13} is large (Tab. 7). Another possibility to establish the presence of Earth effects is to use the signal from two detectors if one of them sees the SN shadowed by the Earth and the other not. A comparison between the signal normalization in the two detectors might reveal Earth effects [81]. The probability for observing a Galactic SN shadowed by the Earth as a function of the detector's geographic latitude depends only mildly on details of the Galactic SN distribution [82]. A location at the North Pole would be optimal with a shadowing probability of about 60%, but a far-northern location such as Pyhäsalmi in Finland, the proposed site for LENA, is almost equivalent (58%). One particular scenario consists of a large-volume scintillator detector located in Pyhäsalmi to measure the geo-neutrino flux in a continental location and another detector in Hawaii to measure it in an oceanic location. The probability that only one of them is shadowed exceeds 50% whereas the probability that at least one is shadowed is about 80%.

As an important caveat, we mention that very recently it has been recognized that nonlinear oscillation effects caused by neutrino-neutrino interactions can have a dramatic impact on the neutrino flavor evolution for approximately the first 100 km above the neutrino sphere [83, 84]. The impact of these novel effects and of their observable signatures is currently under investigation. However, from recent numerical simulations [83] and analytical studies [85], it results that the effects of these non-linear effects would produce a spectral swap $\nu_e\bar{\nu}_e \leftarrow \nu_x\bar{\nu}_x$ at $r \lesssim 400$ km, for inverted neutrino mass hierarchy. An would observe a complete spectral swapping in the $\bar{\nu}$ fluxes, while ν spectra would show a peculiar stepwise splitting. These effect would appear also for astonishingly small values of θ_{13}. These new results suggests once more that one needs complementary detection techniques to be sensitive to both neutrino and anti neutrino channels.

Other interesting ideas have been studied in the literature, as the pointing of a SN by neutrinos [86], determining its distance from the deleptonization burst that plays the role of a standard candle [67], an early alert for an SN observatory exploiting the neutrino signal [87], and the detection of neutrinos from the last phases of a presupernova star [88].

So far, we have investigated SN in our Galaxy, but the calculated rate of supernova explosions within a distance of 10 Mpc is about 1/year. Although the number of events from a single explosion at such large distances would be small, the signal could be separated from the background with the condition to observe at least two events within a time window comparable to the neutrino emission time-scale ($\sim$ 10 sec), together with the full energy and time distribution of the events [89]. In the MEMPHYS

Table 7. Summary of the effect of the neutrino properties on ν_e and $\bar{\nu}_e$ signals.

Mass Hierarchy	$\sin^2\theta_{13}$	ν_e neutronization peak	Shock wave	Earth effect
Normal	$\gtrsim 10^{-3}$	Absent	ν_e	$\bar{\nu}_e$
Inverted	$\gtrsim 10^{-3}$	Present	$\bar{\nu}_e$	ν_e
Any	$\lesssim 10^{-5}$	Present	-	both $\bar{\nu}_e$ ν_e

Table 8. DSNB expected rates. The larger numbers of expected signal events are computed with the present limit on the flux by the Super-Kamiokande Collaboration. The smaller numbers are computed for typical models. The background from reactor plants has been computed for specific sites for LENA and MEMPHYS. For MEMPHYS, the Super-Kamiokande background has been scaled by the exposure.

Interaction	Exposure	Energy Window	Signal/Bkgd
GLACIER			
$\nu_e + {}^{40}Ar \rightarrow e^- + {}^{40}K^*$	0.5 Mton year 5 years	$[16-40]$ MeV	(40-60)/30
LENA at Pyhäsalmi			
$\bar{\nu}_e + p \rightarrow n + e^+$ $n + p \rightarrow d + \gamma$ (2 MeV, 200 μs)	0.4 Mton year 10 years	$[9.5-30]$ MeV	(20-230)/8
1 MEMPHYS module + 0.2% Gd (with bkgd at Kamioka)			
$\bar{\nu}_e + p \rightarrow n + e^+$ $n + Gd \rightarrow \gamma$ (8 MeV, 20 μs)	0.7 Mton year 5 years	$[15-30]$ MeV	(43-109)/47

detector, with at least two neutrinos observed, a SN could be identified without optical confirmation, so that the start of the light curve could be forecast by a few hours, along with a short list of probable host galaxies. This would also allow the detection of supernovae which are either heavily obscured by dust or are optically faint due to prompt black hole formation.

5.2. Diffuse supernova neutrino background

As mentioned above, a galactic SN explosion would be a spectacular source of neutrinos, so that a variety of neutrino and SN properties could be assessed. However, only one such explosion is expected in 20 to 100 years by now. Waiting for the next galactic SN, one can detect the cumulative neutrino flux from all the past SN in the Universe, the so-called Diffuse Supernova Neutrino Background (DSNB). In particular, there is an energy window around $10-40$ MeV where the DSNB signal can emerge above other sources, so that the proposed detectors may well measure this flux after some years of exposure.

The DSNB signal, although weak, is not only guaranteed, but can also allow probing physics different from that of a galactic SN, including processes which occur on cosmological scales in time or space. For instance, the DSNB signal is sensitive to the evolution of the SN rate, which in turn is closely related to the star formation

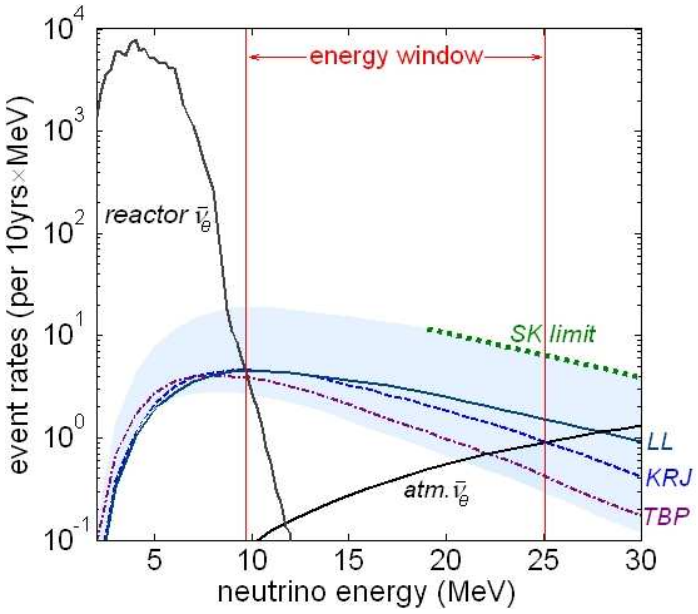

Figure 8. DSNB signal and background in the LENA detector in 10 years of exposure. The shaded regions give the uncertainties of all curves. An observational window between ~ 9.5 to 25 MeV that is almost free of background can be identified (for the Pyhäsalmi site). The DSN neutrino rates are shown for different models of core-collapse supernova simulation performed by the Lawrence Livermore (LL) , Keil, Raffelt and Janka (KRJ) and Thompson, Burrows and Pinto (TBP) groups. Reprinted figure with permission from [40].

rate [90, 91]. In addition, neutrino decay scenarios with cosmological lifetimes could be analyzed and constrained [92] as proposed in [93]. An upper limit on the DSNB flux has been set by the Super-Kamiokande experiment [94]

$$\phi_{\bar{\nu}_e}^{\mathrm{DSNB}} < 1.2 \text{ cm}^{-2} \text{ s}^{-1} (E_\nu > 19.3 \text{ MeV}). \quad (3)$$

An upper limit based on the non observation of distortions of the expected background spectra in the same energy range. The most recent theoretical estimates (see for example [95, 96]) predict a DSNB flux very close to the SK upper limit, suggesting that the DSNB is on the verge of the detection if a significant background reduction is achieved such as Gd loading [41]. With a careful reduction of backgrounds, the proposed large detectors would not only be able to detect the DSNB, but to study its spectral properties with some precision. In particular, MEMPHYS and LENA would be sensitive mostly to the $\bar{\nu}_e$ component of DSNB, through $\bar{\nu}_e$ IBD, while GLACIER would probe ν_e flux, trough $\nu_e + {}^{40}Ar \rightarrow e^- + {}^{40}K^*$ (and the associated gamma cascade) [97].

The DSNB signal energy window is constrained from above by the atmospheric neutrinos and from below by either the nuclear reactor $\bar{\nu}_e$ (I), the spallation production of unstable radionuclei by cosmic-ray muons (II), the decay of "invisible" muons into electrons (III), solar ν_e neutrinos (IV), and low energy atmospheric ν_e and $\bar{\nu}_e$ neutrinos interactions (V). The three detectors are affected differently by these backgrounds. GLACIER looking at ν_e is mainly affected by types IV and V. MEMPHYS filled with

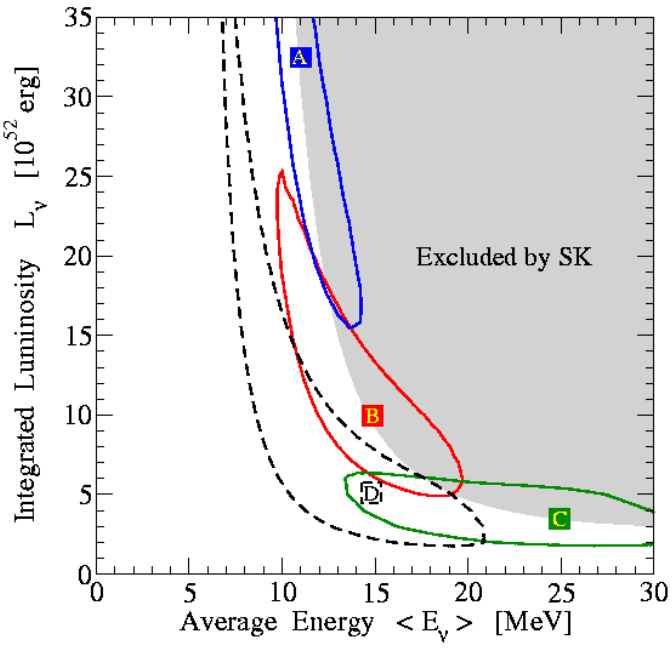

Figure 9. Possible 90% C.L. measurements of the emission parameters of supernova electron antineutrino emission after 5 years running of a Gadolinium-enhanced SK detector or 1 year of one Gadolinium-enhanced MEMPHYS tanks. Reprinted figure with permission from [98].

pure water is affected by types I, II, V and III due to the fact that the muons may not have enough energy to produce Cherenkov light. As pointed out in [72], with the addition of Gadolinium [41] the detection of the captured neutron releasing 8 MeV gamma after ~ 20 μs (10 times faster than in pure water) would give the possibility to reject the "invisible" muon (type III) as well as the spallation background (type II). LENA taking benefit from the delayed neutron capture in $\bar{\nu}_e + p \rightarrow n + e^+$, is mainly concerned with reactor neutrinos (I), which impose to choose an underground site far from nuclear plants. If LENA was installed at the Center for Underground Physics in Pyhäsalmi (CUPP, Finland), there would be an observational window from ~ 9.7 to 25 MeV that is almost free of background. The expected rates of signal and background are presented in Tab. 8. According to current DSNB models [91] that are using different SN simulations ([99, 100, 101]) for the prediction of the DSNB energy spectrum and flux, the detection of $\sim$10 DSNB events per year is realistic for LENA. Signal rates corresponding to different DSNB models and the background rates due to reactor and atmospheric neutrinos are shown in Fig. 8 for 10 years exposure at CUPP.

Apart from the mere detection, spectroscopy of DSNB events in LENA will constrain the parameter space of core-collapse models. If the SN rate signal is known with sufficient precision, the spectral slope of the DSNB can be used to determine the hardness of the initial SN neutrino spectrum. For the currently favoured value of the SN rate, the discrimination between core-collapse models will be possible at 2.6σ after 10 years of measuring time [40]. In addition, by the analysis of the flux in the energy region from 10 to 14 MeV the SN rate for $z < 2$ could be constrained with

high significance, as in this energy regime the DSNB flux is only weakly dependent on the assumed SN model. The detection of the redshifted DSNB from $z > 1$ is limited by the flux of the reactor $\bar{\nu}_e$ background. In Pyhäsalmi, a lower threshold of 9.5 MeV resuls in a spectral contribution of 25% DSNB from $z > 1$.

The analysis of the expected DSNB spectrum that would be observed with a Gadolinium-loaded water Cherenkov detector has been carried out in [98]. The possible measurements of the parameters (integrated luminosity and average energy) of SN $\bar{\nu}_e$ emission have been computed for 5 years running of a Gd-enhanced Super-Kamiokande detector, which would correspond to 1 year of one Gd-enhanced MEMPHYS tank. The results are shown in Fig. 9. Even if detailed studies on the characterization of the background are needed, the DSNB events provide the first neutrino detection originating from cosmological distances.

6. Solar neutrinos

In the past years water Cherenkov detectors have measured the high energy tail ($E > 5$ MeV) of the solar ^{8}B neutrino flux using electron-neutrino elastic scattering [8]. Since such detectors could record the time of an interaction and reconstruct the energy and direction of the recoiling electron, unique information on the spectrum and time variation of the solar neutrino flux were extracted. This provided further insights into the "solar neutrino problem", the deficit of the neutrino flux (measured by several experiments) with respect to the flux expected by solar models, contributing to the assessment of the oscillation scenario for solar neutrinos [4, 5, 6, 7, 8, 9, 10] .

With MEMPHYS, Super-Kamiokande's measurements obtained from 1258 days of data taking could be repeated in about half a year, while the seasonal flux variation measurement will obviously require a full year. In particular, the first measurement of the flux of the rare *hep* neutrinos may be possible. Elastic neutrino-electron scattering is strongly forward peaked. In order to separate the solar neutrino signal from the isotropic background events (mainly due to low radioactivity), this directional correlation is exploited, although the angular resolution is limited by multiple scattering. The reconstruction algorithms first reconstruct the vertex from the PMT timing information and then the direction, by assuming a single Cherenkov cone originating from the reconstructed vertex. Reconstructing 7 MeV events in MEMPHYS seems not to be a problem, but decreasing this threshold would imply serious consideration of the PMT dark current rate as well as the laboratory and detector radioactivity level.

With LENA, a large amount of neutrinos from ^{7}Be (around $\sim 5.4 \times 10^3$/day, $\sim 2.0 \times 10^6$/year) would be detected. Depending on the signal to background ratio, this could provide a sensitivity to time variations in the ^{7}Be neutrino flux of $\sim 0.5\%$ during one month of measuring time. Such a sensitivity can give unique information on helioseismology (pressure or temperature fluctuations in the center of the Sun) and on a possible magnetic moment interaction with a timely varying solar magnetic field. The *pep* neutrinos are expected to be recorded at a rate of 210/day ($\sim 7.7 \times 10^4$/y). These events would provide a better understanding of the global solar neutrino luminosity, allowing to probe (due to their peculiar energy) the transition region of vacuum to matter-dominated neutrino oscillation.

The neutrino flux from the CNO cycle is theoretically predicted with a large uncertainty (30%). Therefore, LENA would provide a new opportunity for a detailed study of solar physics. However, the observation of such solar neutrinos in these

detectors, *i.e.* through elastic scattering, is not a simple task, since neutrino events cannot be separated from the background, and it can be accomplished only if the detector contamination will be kept very low [102, 103]. Moreover, only mono-energetic sources as those mentioned can be detected, taking advantage of the Compton-like shoulder edge produced in the event spectrum.

Recently, the possibility to detect ^{8}B solar neutrinos by means of charged-current interaction with the ^{13}C [104] nuclei naturally contained in organic scintillators has been investigated. Even if signal events do not keep the directionality of the neutrino, they can be separated from background by exploiting the time and space coincidence with the subsequent decay of the produced ^{13}N nuclei. The residual background amounts to about 60/year corresponding to a reduction factor of $\sim 3 \times 10^{-4}$ [104]. Around 360 events of this type per year can be estimated for LENA. A deformation due to the MSW matter effect should be observable in the low-energy regime after a couple of years of measurements.

For the proposed location of LENA in Pyhásalmi ($\sim$ 4000 m.w.e.), the cosmogenic background will produce ^{11}C which contribute to the CNO and pep neutrino measurements. At the Pyhälmi site, the signal to background ratio is estimated to be $\sim$ 1 [105]. Event by event, background rejection can be achieved by registration of the neutron capture which follows ^{11}C production by spallation processes induced by cosmic muons. This technique has been successfully demonstrated in the Counting Test Facility for Borexino (CTF) [106]. Notice that the Fréjus site would also be adequate for this case ($\sim$ 4800 m.w.e.). The radioactivity of the detector would have to be kept very low (10^{-17} g/g level U-Th) as in the KamLAND detector.

Solar neutrinos can be detected by GLACIER through the elastic scattering $\nu_x + e^- \rightarrow \nu_x + e^-$ (ES) and the absorption reaction $\nu_e + {}^{40}Ar \rightarrow e^- + {}^{40}K^*$ (ABS) followed by γ-ray emission. Even if these reactions have low energy threshold (1.5 MeV for the second one), one expects to operate in practice with a threshold set at 5 MeV on the primary electron kinetic energy, in order to reject background from neutron capture followed by gamma emission, which constitutes the main background for some of the underground laboratories [28]. These neutrons are induced by the spontaneous fission and (α,n) reactions in rock. In the case of a salt mine this background can be smaller. The fact that salt has smaller U/Th concentrations does not necessarily mean that the neutron flux is smaller. The flux depends on the rock composition since (alpha,n) reactions may contribute significantly to the flux. The expected raw event rate is 330 000/year (66% from ABS, 25% from ES and 9% from neutron background induced events) assuming the above mentioned threshold on the final electron energy. By applying further offline cuts to purify separately the ES sample and the ABS sample, one obtains the rates shown on Tab. 9.

A possible way to combine the ES and the ABS channels similar to the NC/CC flux ratio measured by SNO collaboration [9], is to compute the following ratio

$$R = \frac{N^{ES}/N_0^{ES}}{\frac{1}{2}\left(N^{Abs-GT}/N_0^{Abs-GT} + N^{Abs-F}/N_0^{Abs-F}\right)} \tag{4}$$

where the numbers N^{ES}, N^{Abs-GT} and N^{Abs-F} are the measured event rates (elastic, absorption Gamow-Teller transition and absorption pure Fermi transition respectively), and the expected events without neutrino oscillations are labeled with a 0). This double ratio has two advantages. First, it is independent of the ^{8}B total neutrino flux, predicted by different solar models, and second, it is free from experimental threshold energy bias and of the adopted cross-sections for the different

Table 9. Number of events expected in GLACIER per year, compared with the computed background (no oscillation) from the Gran Sasso rock radioactivity ($0.32\ 10^{-6}$ n cm^{-2} s^{-1}($>$ 2.5 MeV). The absorption channel has been split into the contributions of events from Fermi and Gamow-Teller transitions of the ^{40}Ar to the different ^{40}K excited levels and that can be separated using the emitted gamma energy and multiplicity.

	Events/year
Elastic channel ($E \geq 5$ MeV)	45 300
Neutron background	1400
Absorption events contamination	1100
Absorption channel (Gamow-Teller transition)	101 700
Absorption channel (Fermi transition)	59 900
Neutron background	5500
Elastic events contamination	1700

channels. With the present fit to solar neutrino experiments and KamLAND data, one expects a value of $R = 1.30 \pm 0.01$ after one year of data taking with GLACIER. The quoted error for R only takes into account statistics.

7. Atmospheric neutrinos

Atmospheric neutrinos originate from the decay chain initiated by the collision of primary cosmic-rays with the upper layers of Earth's atmosphere. The primary cosmic-rays are mainly protons and helium nuclei producing secondary particles such π and K, which in turn decay producing electron- and muon- neutrinos and antineutrinos.

At low energies the main contribution comes from π mesons, and the decay chain $\pi \to \mu + \nu_\mu$ followed by $\mu \to e + \nu_e + \nu_\mu$ produces essentially two ν_μ for each ν_e. As the energy increases, more and more muons reach the ground before decaying, and therefore the ν_μ/ν_e ratio increases. For $E_\nu \gtrsim 1$ GeV the dependence of the total neutrino flux on the neutrino energy is well described by a power law, $d\Phi/dE \propto E^{-\gamma}$ with $\gamma = 3$ for ν_μ and $\gamma = 3.5$ for ν_e, whereas for sub-GeV energies the dependence becomes more complicated because of the effects of the solar wind and of Earth's magnetic field [107]. As for the zenith dependence, for energies larger than a few GeV the neutrino flux is enhanced in the horizontal direction, since pions and muons can travel a longer distance before losing energy in interactions (pions) or reaching the ground (muons), and therefore have more chances to decay producing energetic neutrinos.

Historically, the atmospheric neutrino problem originated in the 80's as a discrepancy between the atmospheric neutrino flux measured with different experimental techniques and the expectations. In the last years, a number of detectors had been built, which could detect neutrinos through the observation of the charged lepton produced in charged-current neutrino-nucleon interactions inside the detector material. These detectors could be divided into two classes: *iron calorimeters*, which reconstruct the track or the electromagnetic shower induced by the lepton, and *water Cherenkov*, which measure the Cherenkov light emitted by the lepton as it moved faster than light in water filling the detector volume. The first iron calorimeters, Frejus [18] and NUSEX [14], found no discrepancy between the observed flux and the theoretical predictions, whereas the two water Cherenkov detectors, IMB [17] and

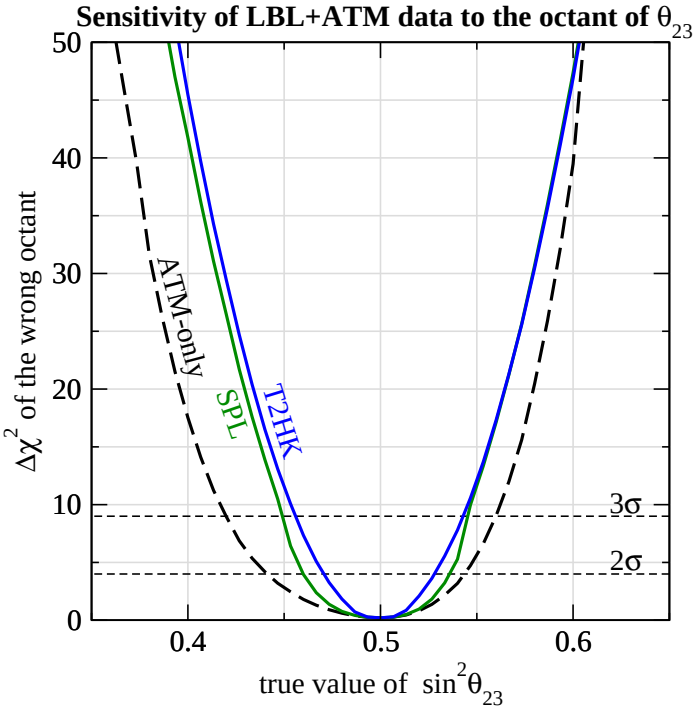

Figure 10. Discrimination of the wrong octant solution as a function of $\sin^2\theta_{23}^{\rm true}$, for $\theta_{13}^{\rm true}=0$. We have assumed 10 years of data taking with a 440 kton detector. Reprinted figure with permission from [37].

Kamiokande [16], observed a clear deficit compared to the predicted ν_μ/ν_e ratio. The problem was finally solved in 1998, when the already mentioned water Cherenkov Super-Kamiokande detector [21] allowed to establish with high statistical accuracy that there was indeed a zenith- and energy-dependent deficit in the muon-neutrino flux with respect to the theoretical predictions, and that this deficit was compatible with the hypothesis of $\nu_\mu \rightarrow \nu_\tau$ oscillations. The independent confirmation of this effect from the calorimeter experiments Soudan-II [19] and MACRO [108] eliminated the original discrepancy between the two experimental techniques.

Despite providing the first solid evidence for neutrino oscillations, atmospheric neutrino experiments suffer from two important limitations. Firstly, the sensitivity of an atmospheric neutrino experiments is strongly limited by the large uncertainties in the knowledge of neutrino fluxes and neutrino-nucleon cross-section. Such uncertainties can be as large as 20%. Secondly, water Cherenkov detectors do not allow an accurate reconstruction of the neutrino energy and direction if none of the two is known a priori. This strongly limits the sensitivity to Δm^2, which is very sensitive to the resolution of L/E.

During its phase-I, Super-Kamiokande has collected 4099 electron-like and 5436 muon-like contained neutrino events [20]. With only about one hundred events each, the accelerator experiments K2K [109] and MINOS [110] already provide a stronger bound on the atmospheric mass-squared difference Δm^2_{31}. The present value of the mixing angle θ_{23} is still dominated by Super-Kamiokande data, being statistically the

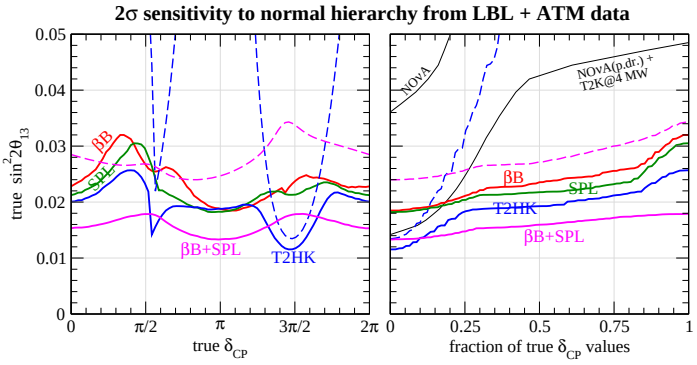

Figure 11. Sensitivity to the mass hierarchy at 2σ ($\Delta\chi^2 = 4$) as a function of $\sin^2 2\theta_{13}^{\rm true}$ and $\delta_{\rm CP}^{\rm true}$ (left), and the fraction of true values of $\delta_{\rm CP}^{\rm true}$ (right). The solid curves are the sensitivities from the combination of long-baseline and atmospheric neutrino data, the dashed curves correspond to long-baseline data only. We have assumed 10 years of data taking with a 440 kton mass detector. Reprinted figure with permission from [37].

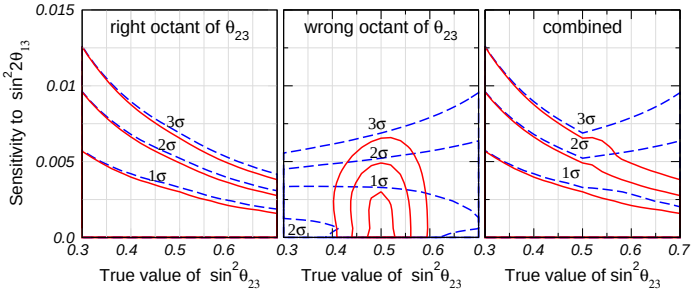

Figure 12. Sensitivity to $\sin^2 2\theta_{13}$ as a function of $\sin^2\theta_{23}^{\rm true}$ for LBL data only (dashed), and the combination beam and atmospheric neutrino data (solid). In the left and central panels we restrict the fit of θ_{23} to the octant corresponding to $\theta_{23}^{\rm true}$ and $\pi/2 - \theta_{23}^{\rm true}$, respectively, whereas the right panel shows the overall sensitivity taking into account both octants. We have assumed 8 years of beam and 9 years of atmospheric neutrino data taking with the T2HK beam and a 1 Mton detector. Reprinted figure with permission from [113].

most important factor for such a measurement. However, large improvements are expected from the next generation of long-baseline experiments such as T2K [111] and NOνA [112], sensitive to the same oscillation parameters as atmospheric neutrino experiments.

Despite the above limitations, atmospheric neutrino detectors can still play a leading role in the future of neutrino physics due to the huge range in energy (from 100 MeV to 10 TeV and above) and distance (from 20 km to more than 12 000 km) covered by the data. This unique feature, as well as the very large statistics expected for a detector such as MEMPHYS ($20 \div 30$ times the present Super-Kamiokande event rate), will allow a very accurate study of the subdominant modification to the leading oscillation pattern, thus providing complementary information to accelerator-based experiments. More concretely, atmospheric neutrino data will be extremely valuable

for

- Resolving the octant ambiguity. Although future accelerator experiments are expected to considerably improve the measurement of the absolute value of the small quantity $D_{23} \equiv \sin^2\theta_{23} - 1/2$, they will have practically no sensitivity on its sign. On the other hands, it has been pointed out [114, 115] that the $\nu_\mu \to \nu_e$ conversion signal induced by the small but finite value of Δm^2_{21} can resolve this degeneracy. However, observing such a conversion requires a very long baseline and low energy neutrinos, and atmospheric sub-GeV electron-like events are particularly suitable for this purpose. In Fig. 10 we show the potential of different experiments to exclude the octant degenerate solution.
- Resolving the hierarchy degeneracy. If θ_{13} is not too small, matter effect will produce resonant conversion in the $\nu_\mu \leftrightarrow \nu_e$ channel for neutrinos (antineutrinos) if the mass hierarchy is normal (inverted). The observation of this enhanced conversion would allow the determination of the mass hierarchy. Although a magnetized detector would be the best solution for this task, it is possible to extract useful information also with a conventional detector since the event rates expected for atmospheric neutrinos and antineutrinos are quite different. This is clearly visible from Fig. 11, where we show how the sensitivity to the mass hierarchy of different beam experiments is drastically increased when the atmospheric neutrino data collected by the same detector are also included in the fit.
- Measuring or improving the bound on θ_{13}. Although atmospheric data alone are not expected to be competitive with the next generation of long-baseline experiments in the sensitivity to θ_{13}, they will contribute indirectly by eliminating the octant degeneracy, which is an important source of uncertainty for beam experiments. In particular, if $\theta_{23}^{\rm true}$ is larger than 45° then the inclusion of atmospheric data will considerably improve the accelerator experiment sensitivity to θ_{13}, as can be seen from the right panel of Fig. 12 [113].

In GLACIER, the search for ν_τ appearance is based on the information provided by the event kinematics and takes advantage of the special characteristics of ν_τ CC and the subsequent decay of the produced τ lepton when compared to CC and NC interactions of ν_μ and ν_e, i.e. by making use of $\vec{P}_{candidate}$ and $\vec{P}_{hadron}$. Due to the large background induced by atmospheric muon and electron neutrinos and antineutrinos, the measurement of a statistically significant excess of ν_τ events is very unlikely for the $\tau \to e$ and $\tau \to \mu$ decay modes.

The situation is much more advantageous for the hadronic channels. One can consider tau-decays to one prong (single pion, ρ) and to three prongs ($\pi^\pm\pi^0\pi^0$ and three charged pions). In order to select the signal, one can exploit the kinematical variables $E_{visible}$, y_{bj} (the ratio between the total hadronic energy and $E_{visible}$) and Q_T (defined as the transverse momentum of the τ candidate with respect to the total measured momentum) that are not completely independent one from another but show some correlation. These correlations can be exploited to reduce the background. In order to maximize the separation between signal and background, one can use three dimensional likelihood functions $\mathcal{L}(Q_T, E_{visible}, y_{bj})$ where correlations are taken into account. For each channel, three dimensional likelihood functions are built for both signal ($\mathcal{L}^S_\pi,\ \mathcal{L}^S_\rho,\ \mathcal{L}^S_{3\pi}$) and background ($\mathcal{L}^B_\pi,\ \mathcal{L}^B_\rho,\ \mathcal{L}^B_{3\pi}$). In order to enhance the separation of ν_τ induced events from $\nu_\mu,\ \nu_e$ interactions, the ratio of likelihoods is taken as the sole discriminant variable $\ln\lambda_i \equiv \ln(\mathcal{L}^S_i/\mathcal{L}^B_i)$ where $i = \pi,\ \rho,\ 3\pi$.

Table 10. Expected GLACIER background and signal events for different combinations of the π, ρ and 3π analyses. The considered statistical sample corresponds to an exposure of 100 kton year.

$\ln\lambda_\pi$ Cut	$\ln\lambda_\rho$ Cut	$\ln\lambda_{3\pi}$ Cut	Top Events	Bottom Events	P_β (%)
0.0	0.5	0.0	223	$223+43=266$	2×10^{-1} (3.1σ)
1.5	1.5	0.0	92	$92+35=127$	2×10^{-2} (3.7σ)
3.0	-1.0	0.0	87	$87+33=120$	3×10^{-2} (3.6σ)
3.0	0.5	0.0	25	$25+22=47$	2×10^{-3} (4.3σ)
3.0	1.5	0.0	20	$20+19=39$	4×10^{-3} (4.1σ)
3.0	0.5	-1.0	59	$59+30=89$	9×10^{-3} (3.9σ)
3.0	0.5	1.0	18	$18+17=35$	1×10^{-2} (3.8σ)

To further improve the sensitivity of the ν_τ appearance search, one can combine the three independent hadronic analyses into a single one. Events that are common to at least two analyses are counted only once and a survey of all possible combinations, for a restricted set of values of the likelihood ratios, is performed. Table 10 illustrates the statistical significance achieved by several selected combinations of the likelihood ratios for an exposure equivalent to 100 kton year.

The best combination for a 100 kton year exposure is achieved for the following set of cuts: $\ln\lambda_\pi > 3$, $\ln\lambda_\rho > 0.5$ and $\ln\lambda_{3\pi} > 0$. The expected number of NC background events amounts to 25 (top) while 25+22 = 47 are expected. We use a suitable discriminant variable to enhance the signal to background ratio of the analyses. After cuts, two sets of events are built: n_b (the number of expected downward going background) and $n_t = n_b + n_s$ (the number of expected upward going events, where n_s is the number of taus). A statistical treatment of the data is performed by building two Poissonian probability density functions:

$$f_b(r) \equiv \frac{e^{-n_b} n_b^r}{r!} \tag{5}$$

with mean n_b and

$$f_t(r) \equiv \frac{e^{-n_t} n_t^r}{r!} \tag{6}$$

with mean n_t. The statistical significance of the expected n_s excess is evaluated following two procedures:

- The pdf f_b and f_t are integrated over the whole spectrum of possible measured r values and the overlap between the two is computed: $P_\alpha \equiv \int_0^\infty min(f_b(r),\ f_t(r))dr$. The smaller the overlap integrated probability (P_α) the larger the significance of the expected excess.
- We compute the probability $P_\beta \equiv \int_{n_t}^\infty \frac{e^{-n_b} n_b^r}{r!} dr$ that, due to a statistical fluctuation of the unoscillated data, we measure n_t events or more when n_b are expected.

As a result, an effect larger than 4σ is obtained for an exposure of 100 kton year (one year of data taking with GLACIER).

Last but not least, it is worth noting that atmospheric neutrino fluxes are themselves an important subject of investigation, and in the light of the precise determination of the oscillation parameters provided by long baseline experiments,

the atmospheric neutrino data accumulated by the proposed detectors could be used as a direct measurement of the incoming neutrino flux, and therefore as an indirect measurement of the primary cosmic-rays flux.

The appearance of subleading features in the main oscillation pattern can also be a hint for New Physics. The huge range of energies probed by atmospheric data will allow to set very strong bounds on mechanisms which predict deviation from the $1/E$ law behavior. For example, the bound on non-standard neutrino-matter interactions and on other types of New Physics (such as violation of the equivalence principle, or violation of the Lorentz invariance) which can be derived from present data is already the strongest which can be put on these mechanisms [116].

8. Geo-neutrinos

The total power dissipated from the Earth (heat flow) has been measured with thermal techniques to be 44.2 ± 1.0 TW. Despite this small quoted error, a more recent evaluation of the same data (assuming much lower hydrothermal heat flow near mid-ocean ridges) has led to a lower figure of 31 ± 1 TW. On the basis of studies of chondritic meteorites the calculated radiogenic power is thought to be 19 TW (about half of the total power), 84% of which is produced by ^{238}U and ^{232}Th decay which in turn produce $\bar{\nu}_e$ by beta-decays (geo-neutrinos). It is then of prime importance to measure the $\bar{\nu}_e$ flux coming from the Earth to get geophysical information, with possible applications in the interpretation of the geomagnetism.

The KamLAND collaboration has recently reported the first observation of the geo-neutrinos [24]. The events are identified by the time and distance coincidence between the prompt e^+ and the delayed (200 μs) neutron capture produced by $\bar{\nu}_e + p \rightarrow n + e^+$ and emiting a 2.2 MeV gamma. The energy window to search for the geo-neutrino events is [1.7, 3.4] MeV. The lower bound corresponds to the reaction threshold while the upper bound is constrained by nuclear reactor induced background events. The measured rate in the 1 kton liquid scintillator detector located at the Kamioka mine, where the Kamiokande detector was previously installed, is 25^{+19}_{-18} for a total background of 127 ± 13 events.

The background is composed by 2/3 of $\bar{\nu}_e$ events from the nuclear reactors in Japan and Korea. These events have been actually used by KamLAND to confirm and precisely measure the Solar driven neutrino oscillation parameters (see Section 6). The residual 1/3 of the events originates from neutrons of 7.3 MeV produced in $^{13}\mathrm{C}(\alpha, n)^{16}\mathrm{O}$ reactions and captured as in the IBD reaction. The α particles come from the ^{210}Po decays, a ^{222}Rn daughter which is of natural radioactivity origin. The measured geo-neutrino events can be converted in a rate of $5.1^{+3.9}_{-3.6} \times 10^{-31}$ $\bar{\nu}_e$ per target proton per year corresponding to a mean flux of $5.7 \times 10^6 \mathrm{cm}^{-2}$ s^{-1}, or this can be transformed into a 99% C.L. upper bound of 1.45×10^{-30} $\bar{\nu}_e$ per target proton per year ($1.62 \times 10^7 \mathrm{cm}^{-2}$ s^{-1} and 60 TW for the radiogenic power).

In LENA at CUPP a geo-neutrino rate of roughly 1000/year [117] from the dominant $\bar{\nu}_e + p \rightarrow e^+ + n$ IBD reaction is expected. The delayed coincidence measurement of the positron and the 2.2 MeV gamma event, following neutron capture on protons in the scintillator provides a very efficient tool to reject background events. The threshold energy of 1.8 MeV allows the measurement of geo-neutrinos from the Uranium and Thorium series, but not from ^{40}K. A reactor background rate of about 240 events per year for LENA at CUPP in the relevant energy window from 1.8 MeV to 3.2 MeV has been calculated. This background can be subtracted statistically using

the information on the entire reactor neutrino spectrum up to $\simeq 8$ MeV.

As it was shown in KamLAND, a serious background source may come from radio impurities. There the correlated background from the isotope ^{210}Po is dominating. However, with an enhanced radiopurity of the scintillator, the background can be significantly reduced. Taking the radio purity levels of the Borexino CTF detector at Gran Sasso, where a ^{210}Po activity of $35 \pm 12/\mathrm{m}^3\mathrm{day}$ in PXE has been observed, this background would be reduced by a factor of about 150 compared to KamLAND and would account to less than 10 events per year in the LENA detector.

An additional background that fakes the geo-neutrino signal is due to ^{9}Li, which is produced by cosmic-muons in spallation reactions with ^{12}C and decays in a β-neutron cascade. Only a small part of the ^{9}Li decays falls into the energy window which is relevant for geo-neutrinos. KamLAND estimates this background to be 0.30 ± 0.05 [24].

At CUPP the muon reaction rate would be reduced by a factor $\simeq 10$ due to better shielding and this background rate should be at the negligible level of $\simeq 1$ event per year in LENA. From these considerations it follows that LENA would be a very capable detector for measuring geo-neutrinos. Different Earth models could be tested with great significance. The sensitivity of LENA for probing the unorthodox idea of a geo-reactor in the Earth's core was estimated, too. At the CUPP underground laboratory the neutrino background with energies up to $\simeq 8$ MeV due to nuclear power plants was calculated to be around 2200 events per year. A 2 TW geo-reactor in the Earth's core would contribute 420 events per year and could be identified at a statistical level of better than 3σ after only one year of measurement.

Finally, in GLACIER the $\bar{\nu}_e + {}^{40}Ar \rightarrow e^+ + {}^{40}Cl^*$ has a threshold of 7.5 MeV, which is too high for geo-neutrino detection.

9. Indirect searches for the Dark Matter of the Universe

The Weakly Interacting Massive Particles (WIMPs) that likely constitute the halo of the Milky Way can occasionally interact with massive objects, such as stars or planets. When they scatter off such an object, they can potentially lose enough energy that they become gravitationally bound and eventually will settle in the center of the celestial body. In particular, WIMPs can be captured by and accumulate in the core of the Sun.

As far as the next generation of large underground observatories is concerned, although not specifically dedicated to the search for WIMP particles, one could discuss the capability of GLACIER in identifying, in a model-independent way, neutrino signatures coming from the products of WIMP annihilations in the core of the Sun [118].

Signal events will consist of energetic electron- (anti)neutrinos coming from the decay of τ leptons and b quarks produced in WIMP annihilation in the core of the Sun. Background contamination from atmospheric neutrinos is expected to be low. One cannot consider the possibility of observing neutrinos from WIMPs accumulated in the Earth. Given the smaller mass of the Earth and the fact that only scalar interactions contribute, the capture rates for our planet are not enough to produce a statistically significant signal in GLACIER.

The search method takes advantage of the excellent angular reconstruction and superb electron identification capabilities GLACIER offers in looking for an excess of energetic electron- (anti)neutrinos pointing in the direction of the Sun. The expected

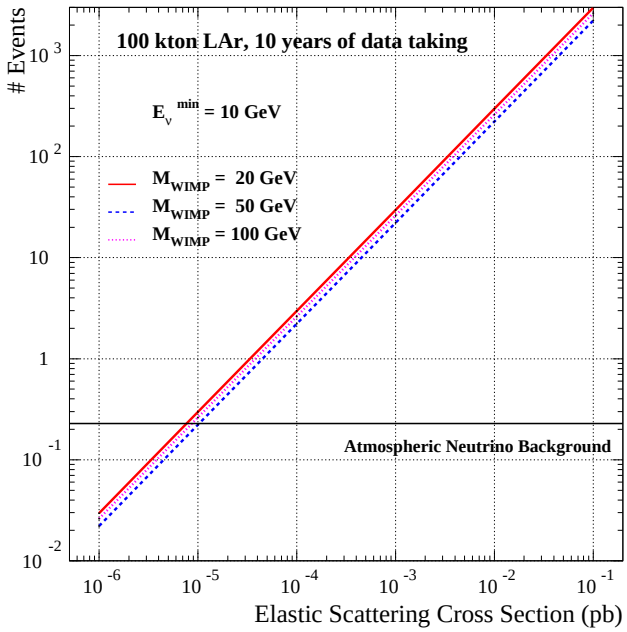

Figure 13. Expected number of signal and background events as a function of the WIMP elastic scattering production cross-section in the Sun, with a cut of 10 GeV on the minimum neutrino energy. Reprinted figure with permission from [118].

signal and background event rates have been evaluated, as said above in a model independent way, as a function of the WIMP elastic scattering cross-section for a range of masses up to 100 GeV. The detector discovery potential, namely the number of years needed to claim a WIMP signal has been discovered, is shown in Figs. 13 and 14. With the assumed set-up and thanks to the low background environment provided by the LAr TPC, a clear WIMP signal would be detected provided the elastic scattering cross-section in the Sun is above $\sim 10^{-4}$ pb.

10. Neutrinos from nuclear reactors

The KamLAND 1 kton liquid scintillator detector located at Kamioka measured the neutrino flux from 53 power reactors corresponding to 701 Joule/cm^2 [26]. An event rate of 365.2 ± 23.7 above 2.6 MeV for an exposure of 766 ton year from the nuclear reactors was expected. The observed rate was 258 events with a total background of 17.8 ± 7.3. The significant deficit combined with the solar experiment results, interpreted in terms of neutrino oscillations, enables a measurement of θ_{12}, the neutrino 1-2 family mixing angle ($\sin^2\theta_{12} = 0.31^{+0.02}_{-0.03}$) as well as the mass squared difference $\Delta m^2_{12} = (7.9 \pm 0.3) \times 10^{-5}\text{eV}^2$.

Future precision measurements are currently being investigated. Running KamLAND for 2-3 more years would gain 30% (4%) reduction in the spread of Δm^2_{12} (θ_{12}). Although it has been shown in Sections 5 and 8 that $\bar{\nu}_e$ originated from nuclear

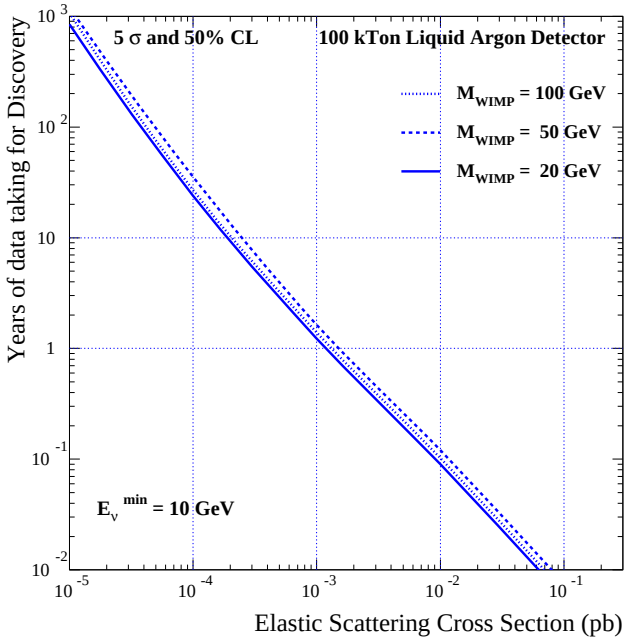

Figure 14. Minimum number of years required to claim a discovery WIMP signal from the Sun in a 100 kton LAr detector as function of $\sigma_{\rm elastic}$ for three values of the WIMP mass. Reprinted figure with permission from [118].

reactors can be a serious background for diffuse supernova neutrino and geo-neutrino detection, the Fréjus site can take benefit of the nuclear reactors located in the Rhône valley to measure Δm^2_{21} and $\sin^2\theta_{12}$. In fact, approximately 67% of the total reactor $\bar{\nu}_e$ flux at Fréjus originates from four nuclear power plants in the Rhone valley, located at distances between 115 km and 160 km. The indicated baselines are particularly suitable for the study of the $\bar{\nu}_e$ oscillations driven by Δm^2_{21}. The authors of [119] have investigated the possibility of using one module of MEMPHYS (147 kton fiducial mass) doped with Gadolinium or the LENA detector, updating the previous work of [120]. Above 3 MeV (2.6 MeV) the event rate is 59 980 (16 670) events/year for MEMPHYS (LENA), which is 2 orders of magnitude larger than the KamLAND event rate.

In order to test the sensitivity of the experiments, the prompt energy spectrum is subdivided into 20 bins between 3 MeV and 12 MeV for MEMPHYS-Gd and Super-Kamiokande-Gd, and into 25 bins between 2.6 MeV and 10 MeV for LENA (Fig. 15). A χ^2 analysis taking into account the statistical and systematical errors shows that each of the two detectors, MEMPHYS-Gd and LENA if placed at Fréjus, can be exploited to yield a precise determination of the solar neutrino oscillation parameters Δm^2_{21} and $\sin^2\theta_{12}$. Within one year, the 3σ uncertainties on Δm^2_{21} and $\sin^2\theta_{12}$ can be reduced respectively to less than 3% and to approximately 20% (Fig. 16). In comparison, the Gadolinium doped Super-Kamiokande detector that might be envisaged in a near future would reach a similar precision only with a much longer data taking time.

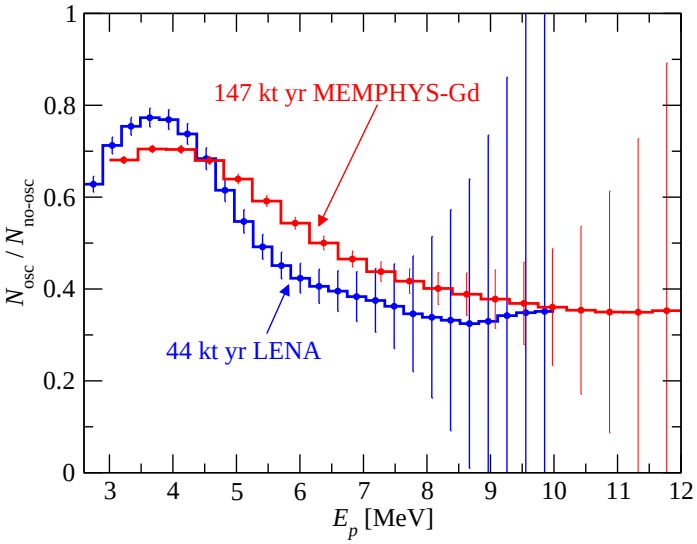

Figure 15. The ratio of the event spectra in positron energy in the case of oscillations with $\Delta m^2_{21} = 7.9 \times 10^{-5}$ eV^2 and $\sin^2\theta_{12} = 0.30$ and in the absence of oscillations, determined using one year data of MEMPHYS-Gd and LENA located at Frejus. The error bars correspond to 1σ statistical error. Reprinted figure with permission from [119].

Several years of reactor $\bar{\nu}_e$ data collected by MEMPHYS-Gd or LENA would allow a determination of Δm^2_{21} and $\sin^2\theta_{12}$ with uncertainties of approximately 1% and 10% at 3σ, respectively.

However, some caveat are worth to be mentioned. The prompt energy trigger of 3 MeV requires a very low PMT dark current rate in the case of the MEMPHYS detector. If the energy threshold is higher, the parameter precision decreases as can be seen in Fig. 17. The systematic uncertainties are also an important factor in the experiments under consideration, especially the determination of the mixing angle, as those on the energy scale and the overall normalization.

Anyhow, the accuracy in the knowledge of the solar neutrino oscillation parameters, which can be obtained in the high statistics experiments considered here, are comparable to those that can be reached for the atmospheric neutrino oscillation parameters Δm^2_{31} and $\sin^2\theta_{23}$ with the future long-baseline Super beam experiments such as T2HK or T2KK [121] in Japan, or SPL from CERN to MEMPHYS. Hence, such reactor measurements would complete the program of the high precision determination of the leading neutrino oscillation parameters.

11. Neutrinos from particle accelerator beams

Although the main physics goals of the proposed liquid-based detectors will be in the domain of astro-particle physics, it would be economical and also very interesting from the physics point of view, considering their possible use as "far" detectors for the future neutrino facilities planned or under discussion in Europe, also given the large financial investment represented by the detectors. In this Section we review the physics program of the proposed observatories when using different accelerator

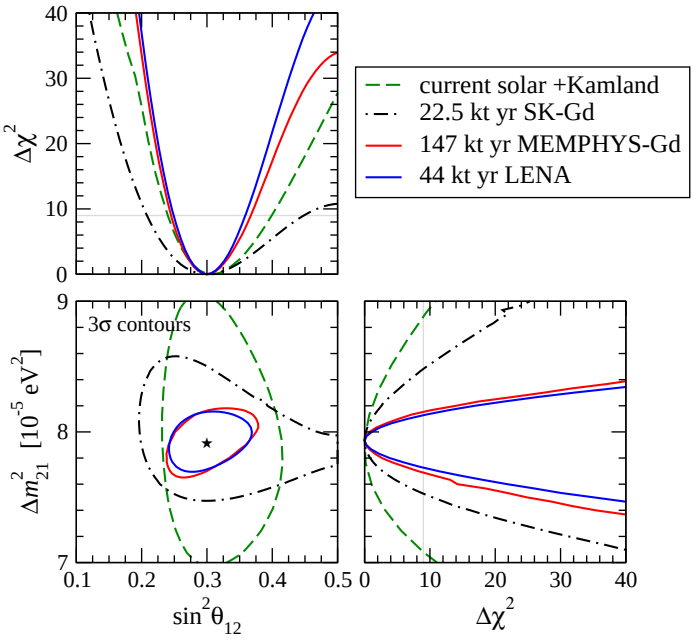

Figure 16. Accuracy of the determination of Δm^2_{21} and $\sin^2\theta_{12}$, for one year data taking of MEMPHYS-Gd and LENA at Frejus, and Super-Kamiokande-Gd, compared to the current precision from solar neutrino and KamLAND data. The allowed regions at 3σ (2 d.o.f.) in the $\Delta m^2_{21} - \sin^2\theta_{12}$ plane, as well as the projections of the χ^2 for each parameter are shown. Reprinted figure with permission from [119].

neutrino beams. The main goals will be pushing the search for a non-zero (although very small) θ_{13} angle or its measurement in the case of a discovery previously made by one of the planned reactor or accelerator experiments (Double-CHOOZ or T2K); searching for possible leptonic CP violation ($\delta_{\rm CP}$); determining the mass hierarchy (the sign of Δm^2_{31}) and the θ_{23} octant ($\theta_{23} > 45°$ or $\theta_{23} < 45°$). For this purpose we consider here the potentiality of a liquid Argon detector in an upgraded version of the existing CERN to Gran Sasso (CNGS) neutrino beam, and of the MEMPHYS detector at the Fréjus using a possible new CERN proton driver (SPL) to upgrade to 4 MW the conventional neutrino beams (Super Beams). Another scheme contemplates a pure electron- (anti)neutrino production by radioactive ion decays (Beta Beam). Note that LENA is also a good candidate detector for the latter beam option. Finally, as an ultimate beam facility, one may think of producing very intense neutrino beams by means of muon decays (Neutrino Factory) that may well be detected with a liquid Argon detector such as GLACIER.

The determination of the missing U_{e3} (θ_{13}) element of the neutrino mixing matrix is possible via the detection of $\nu_\mu \rightarrow \nu_e$ oscillations at a baseline L and energy E given by the atmospheric neutrino signal, corresponding to a mass squared difference $E/L \sim \Delta m^2 \simeq 2.5 \times 10^{-3}\ eV^2$. The current layout of the CNGS beam from CERN to the Gran Sasso Laboratory has been optimized for a τ-neutrino appearance search to be performed by the OPERA experiment [122]. This beam configuration provides limited sensitivity to the measurement of U_{e3}.

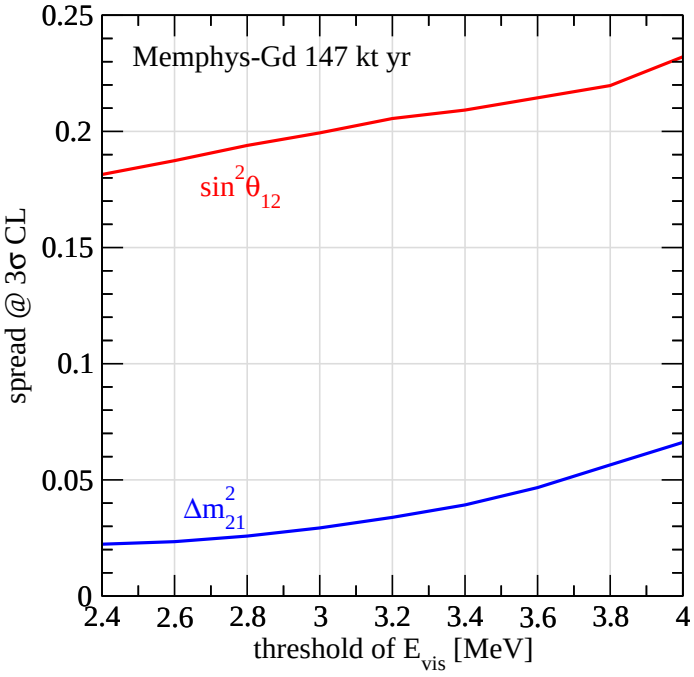

Figure 17. The accuracy of the determination of Δm^2_{21} and $\sin^2\theta_{12}$, which can be obtained using one year of data from MEMPHYS-Gd as a function of the prompt energy threshold.

Therefore, we discuss the physics potential of an intensity-upgraded and energy-reoptimized CNGS neutrino beam coupled to an off-axis GLACIER detector [123]. This idea is based on the possible upgrade of the CERN PS or on a new machine (PS+) to deliver protons of 50 GeV/c with a power of 200 kW. Post acceleration to SPS energies followed by extraction to the CNGS target region should allow to reach MW power, with neutrino energies peaked around 2 GeV. In order to evaluate the physics potential one assumes five years of running in the neutrino horn polarity plus five additional years in the anti-neutrino mode. A systematic error on the knowledge of the ν_e component of 5% is assumed. Given the excellent π^0 particle identification capabilities of GLACIER, the contamination of π^0 is negligible.

An off-axis beam search for ν_e appearance is performed with the GLACIER detector located at 850 km from CERN. For an off-axis angle of 0.75^o, θ_{13} can be discovered for full δ_{CP} coverage for $\sin^2 2\theta_{13} > 0.004$ at 3σ (Fig. 18). At this rather modest baseline, the effect of CP violation and matter effects cannot be disentangled. In fact, the determination of the mass hierarchy with half-coverage (50%) is reached only for $\sin^2 2\theta_{13} > 0.03$ at 3σ. A longer baseline (1050 km) and a larger off-axis angle (1.5^o) would allow the detector to be sensitive to the first minimum and the second maximum of the oscillation. This is the key to resolve the issue of mass hierarchy. With this detector configuration, full coverage for δ_{CP} to determine the mass hierarchy can be reached for $\sin^2 2\theta_{13} > 0.04$ at 3σ. The sensitivity to mass hierarchy determination can be improved by considering two off-axis detectors: one of 30 kton at 850 km and off-axis angle 0.75^o, a second one of 70 kton at 1050 km and 1.5^0 off-axis. Full

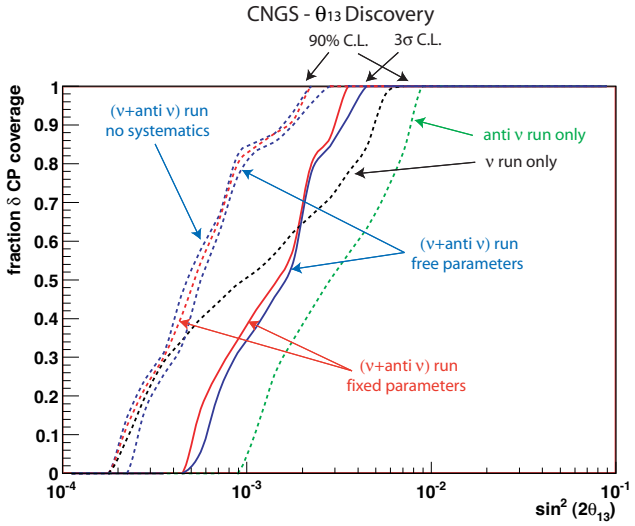

Figure 18. GLACIER in the upgraded CNGS beam. Sensitivity to the discovery of θ_{13}: fraction of δ_{CP} coverage as a function of $\sin^2 2\theta_{13}$. Reprinted figure with permission from [123].

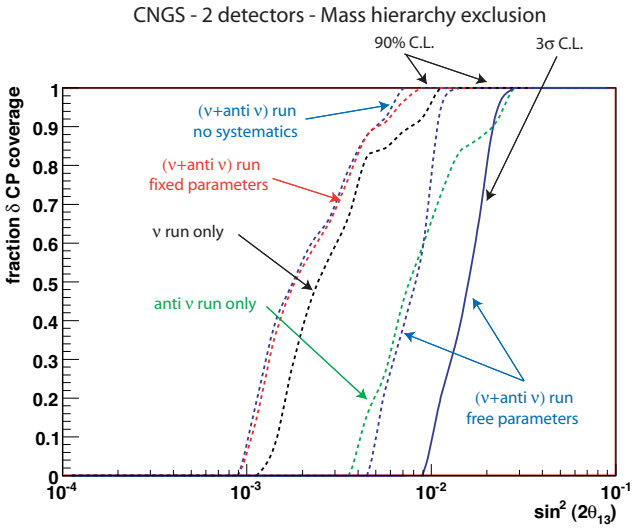

Figure 19. Upgraded CNGS beam: mass hierarchy determination for a two detector configuration at baselines of 850 km and 1050 km. Reprinted figure with permission from [123].

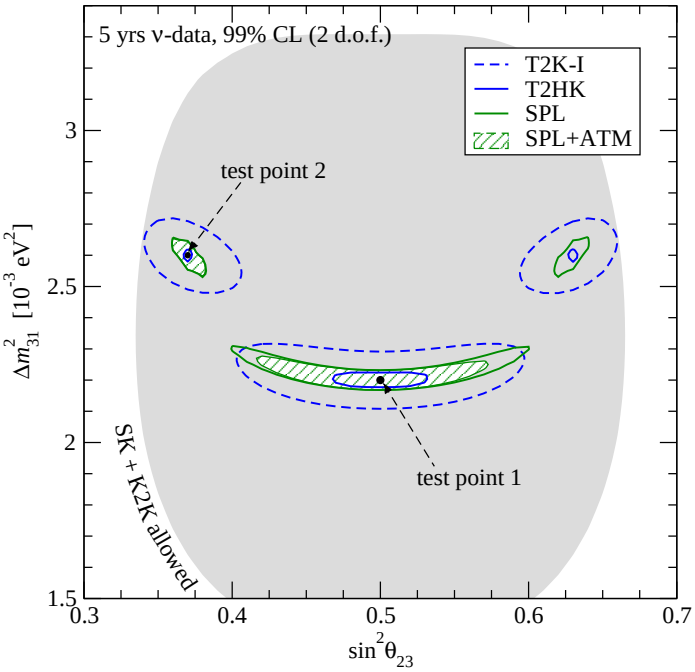

Figure 20. Allowed regions of Δm^2_{31} and $\sin^2\theta_{23}$ at 99% C.L. (2 d.o.f.) after 5 years of neutrino data taking for ATM+SPL, T2K phase I, ATM+T2HK, and the combination of SPL with 5 years of atmospheric neutrino data in the MEMPHYS detector. For the true parameter values we use $\Delta m^2_{31} = 2.2\,(2.6) \times 10^{-3}$ eV^2 and $\sin^2\theta_{23} = 0.5\,(0.37)$ for the test point 1 (2), and $\theta_{13} = 0$ and the solar parameters as: $\Delta m^2_{21} = 7.9 \times 10^{-5}$ eV^2, $\sin^2\theta_{12} = 0.3$. The shaded region corresponds to the 99% C.L. region from present SK and K2K data [124]. Reprinted figure with permission from [37].

coverage for δ_{CP} to determine the mass hierarchy can be reached for $\sin^2 2\theta_{13} > 0.02$ at 3σ (Fig. 19). This two-detector configuration reaches very similar sensitivities to the ones of the T2KK proposal [121].

Another notable possibility is the CERN-SPL Super Beam project. It is a conventional neutrino beam featuring a 4 MW SPL (Super-conducting Proton Linac) [125] driver delivering protons onto a liquid Mercury target to generate an intense π^+ (π^-) beam with small contamination of kaons. The use of near and far detectors will allow both ν_μ disappearance and $\nu_\mu \to \nu_e$ appearance studies. The physics potential of the SPL Super Beam with MEMPHYS has been extensively studied [37, 126, 127]. However, the beam simulations will need some retuning after the forthcoming results of the CERN HARP experiment [128] on hadro-production.

After 5 years exposure in ν_μ disappearance mode, a 3σ accuracy of (3-4)% can be achieved on Δm^2_{31}, and an accuracy of 22% (5%) on $\sin^2\theta_{23}$ if the true value is 0.5 (0.37), namely in case of maximal or non-maximal mixing (Fig. 20). The use of atmospheric neutrinos can contribute to solving the octant ambiguity in case of non-maximal mixing as it is shown in Fig. 20. Note however, that thanks to a higher energy beam ($\sim$ 750 MeV), the T2HK project‡ can benefit from a much lower dependence on

‡ Here, we to the project where a 4 MW proton driver is built at KEK to deliver an intense neutrino

the Fermi motion to obtain a better energy resolution.

In appearance mode (2 years ν_μ plus 8 years $\bar{\nu}_\mu$), a 3σ discovery of non-zero θ_{13}, irrespective of the actual true value of $\delta_{\rm CP}$, is achieved for $\sin^2 2\theta_{13} \gtrsim 4\ 10^{-3}$ ($\theta_{13} \gtrsim 3.6^\circ$) as shown in Fig. 21. For maximal CP violation ($\delta_{\rm CP}^{\rm true} = \pi/2,\ 3\pi/2$) the same discovery level can be achieved for $\sin^2 2\theta_{13} \gtrsim 8\ 10^{-4}$ ($\theta_{13} \gtrsim 0.8^\circ$). The best sensitivity for testing CP violation (*i.e* the data cannot be fitted with $\delta_{\rm CP} = 0$ nor $\delta_{\rm CP} = \pi$) is achieved for $\sin^2 2\theta_{13} \approx 10^{-3}$ ($\theta_{13} \approx 0.9^\circ$) as shown in Fig. 22. The maximum sensitivity is achieved for $\sin^2 2\theta_{13} \sim 10^{-2}$ where the CP violation can be established at 3σ for 73% of all the $\delta_{\rm CP}^{\rm true}$.

Although quite powerful, the proposed SPL Super Beam is a conventional neutrino beam with known limitations due to the low production rate of anti-neutrinos compared to neutrinos which, in addition to a smaller charged-current cross-section, imposes to run 4 times longer in anti-neutrino mode, and implies difficulty to set up an accurate beam simulation, and to design a non-trivial near detector setup mastering the background level. Thus, a new type of neutrino beam, the so-called Beta Beam is being considered. The idea is to generate pure, well collimated and intense $\nu_e(\bar{\nu}_e)$ beams by producing, collecting, and accelerating radioactive ions [129]. The resulting Beta Beam spectra can be easily computed knowing the beta-decay spectrum of the parent ion and the Lorentz boost factor γ, and these beams are virtually free from other background flavors. The best ion candidates so far are ^{18}Ne and ^{6}He for $\nu_e$and $\bar{\nu}_e$, respectively. A baseline study for the Beta Beam has been initiated at CERN, and is now going on within the European FP6 design study for EURISOL.

The potential of such Beta Beam sent to MEMPHYS has been studied in the context of the baseline scenario, using reference fluxes of 5.8×10^{18} ^{6}He useful decays/year and 2.2×10^{18} ^{18}Ne decays/year, corresponding to a reasonable estimate by experts in the field of the ultimately achievable fluxes. The optimal values is actually $\gamma = 100$ for both species, and the corresponding performance have been recently reviewed in [37, 126, 127].

In Figs. 21,22 the results of running a Beta Beam during 10 years (5 years with neutrinos and 5 years with anti-neutrinos) is shown and prove to be far better compared to an SPL Super beam run, especially for maximal CP violation where a non-zero θ_{13} value can be stated at 3σ for $\sin^2 2\theta_{13} \gtrsim 2\ 10^{-4}$ ($\theta_{13} \gtrsim 0.4^\circ$). Moreover, it is noticeable that the Beta Beam is less affected by systematic errors of the background compared to the SPL Super beam and T2HK.

Before combining the two possible CERN beam options, relevant for the proposed European underground observatories, let us consider LENA as potential detector. LENA, with a fiducial volume of $\sim$ 45 kton, can as well be used as detector for a low-energy Beta Beam oscillation experiment. In the energy range $0.2 - 1.2$ GeV, the performed simulations show that muon events are separable from electron events due to their different track lengths in the detector and due to the electron emitted in the muon decay. For high energies, muons travel longer than electrons, as the latter undergo scattering and bremsstrahlung. This results in different distributions of the number of photons and the timing pattern, which can be used to distinguish between the two classes of events. For low energies, muons can be recognized by observing the electron of its succeeding decay after a mean time of 2.2 μs. By using both criteria, an efficiency of $\sim$ 90 % for muon appearance has been calculated with acceptance of 1 % electron background. The advantage of using a liquid scintillator detector for

beam detected by a large water Cherenkov detector.

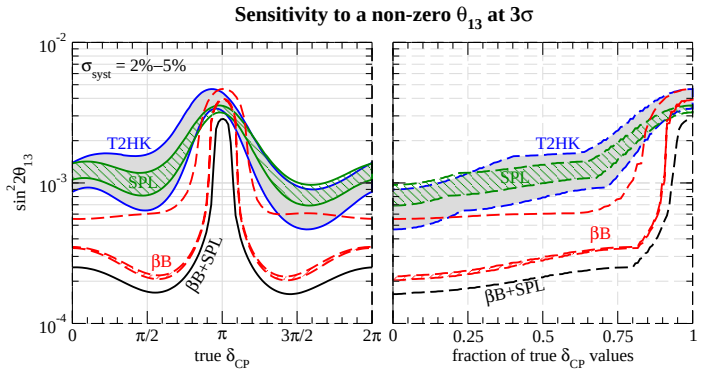

Figure 21. 3σ discovery sensitivity to $\sin^2 2\theta_{13}$ for Beta Beam, SPL, and T2HK as a function of the true value of $\delta_{\rm CP}$ (left panel) and as a function of the fraction of all possible values of $\delta_{\rm CP}$ (right panel). The width of the bands corresponds to values for the systematical errors between 2% and 5%. The dashed curve corresponds to the Beta Beam sensitivity with the fluxes reduced by a factor 2. Reprinted figure with permission from [37].

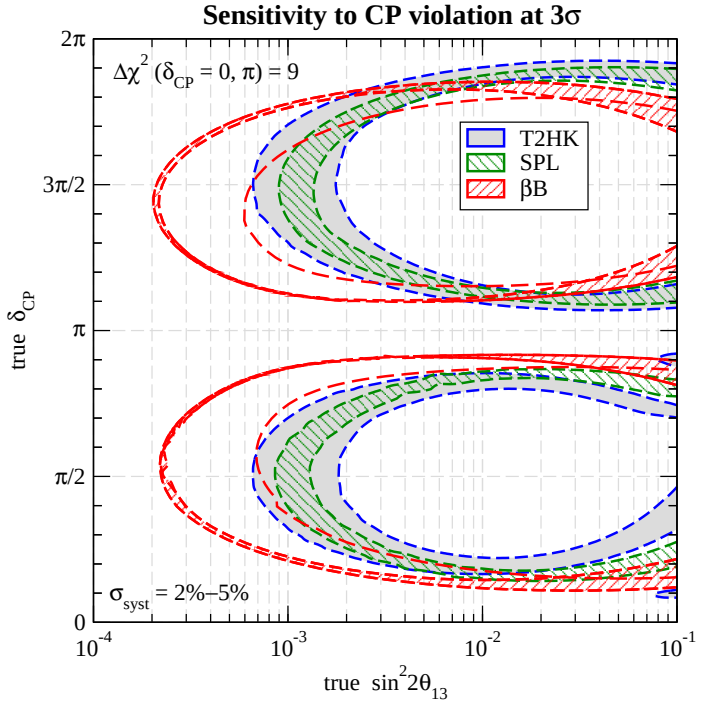

Figure 22. CP violation discovery potential for Beta Beam, SPL, and T2HK: For parameter values inside the ellipse-shaped curves CP conserving values of $\delta_{\rm CP} = 0, \pi$ can be excluded at 3σ ($\Delta\chi^2 > 9$). The width of the bands corresponds to values for the systematic errors from 2% to 5%. The dashed curve is described in Fig. 21. Reprinted figure with permission from [37].

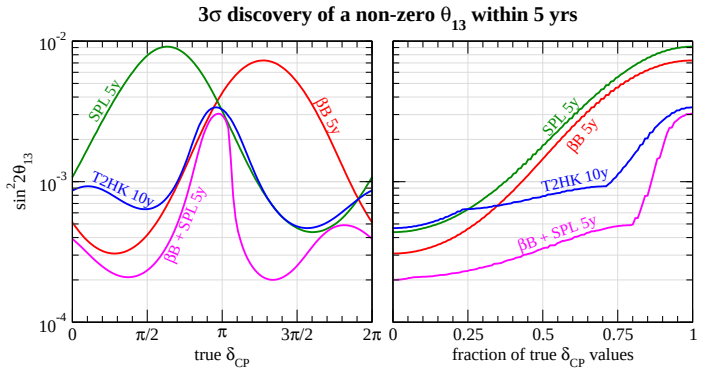

Figure 23. Discovery potential of a finite value of $\sin^2 2\theta_{13}$ at 3σ ($\Delta\chi^2 > 9$) for 5 years neutrino data from Beta Beam, SPL, and the combination of Beta Beam + SPL compared to 10 years data from T2HK (2 years neutrinos + 8 years antineutrinos). Reprinted figure with permission from [37].

such an experiment is the good energy reconstruction of the neutrino beam. However, neutrinos of these energies can produce Δ resonances which subsequently decay into a nucleon and a pion. In water Cherenkov detectors, pions with energies under the Cherenkov threshold contribute to the uncertainty of the neutrino energy. In LENA these particles can be detected. The effect of pion production and similar reactions is currently under investigation in order to estimate the actual energy resolution.

We also mention a very recent development of the Beta Beam concept [38] based on a very promising alternative for the production of ions and on the possibility of having monochromatic, single-flavor neutrino beams by using ions decaying through the electron capture process [130, 131]. In particular, such beams would be suitable to precisely measure neutrino cross-sections in a near detector with the possibility of an energy scan by varying the γ value of the ions. Since a Beta Beam uses only a small fraction of the protons available from the SPL, Super and Beta Beams can be run at the same time. The combination of a Super Beam and a Beta Beam offers advantages from the experimental point of view since the same parameters θ_{13} and δ_{CP} can be measured in many different ways, using 2 pairs of CP related channels, 2 pairs of T related channels, and 2 pairs of CPT related channels which should all give coherent results. In this way, the estimates of systematic errors, different for each beam, will be experimentally cross-checked. Needless to say, the unoscillated data for a given beam will provide a large sample of events corresponding to the small searched-for signal with the other beam, adding more handles to the understanding of the detector response.

The combination of the Beta Beam and the Super Beam will allow to use neutrino modes only: ν_μ for SPL and ν_e for Beta Beam. If CPT symmetry is assumed, all the information can be obtained as $P_{\bar{\nu}_e \to \bar{\nu}_\mu} = P_{\nu_\mu \to \nu_e}$ and $P_{\bar{\nu}_\mu \to \bar{\nu}_e} = P_{\nu_e \to \nu_\mu}$. We illustrate this synergy in Fig. 23. In this scenario, time consuming anti-neutrino running can be avoided keeping the same physics discovery potential.

One can also combine SPL, Beta Beam and the atmospheric neutrino experiments to reduce the parameter degeneracies which lead to disconnected regions on the multi-dimensional space of oscillation parameters. One can look at [132, 133, 134] for the definitions of *intrinsic*, *hierarchy*, and *octant* degeneracies. As we have seen above,

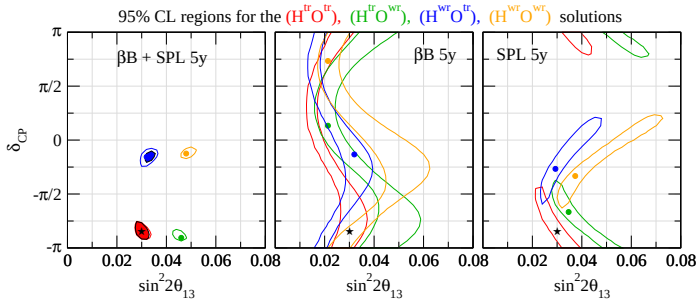

Figure 24. Allowed regions in $\sin^2 2\theta_{13}$ and δ_{CP} for 5 years data (neutrinos only) from Beta Beam, SPL, and the combination. $H^{tr/wr}(O^{tr/wr})$ refers to solutions with the true/wrong mass hierarchy (octant of θ_{23}). For the colored regions in the left panel also 5 years of atmospheric data are included; the solution with the wrong hierarchy has $\Delta\chi^2 = 3.3$. The true parameter values are $\delta_{CP} = -0.85\pi$, $\sin^2 2\theta_{13} = 0.03$, $\sin^2\theta_{23} = 0.6$. For the Beta Beam only analysis (middle panel) an external accuracy of 2% (3%) for $|\Delta m^2_{31}|$ (θ_{23}) has been assumed, whereas for the left and right panel the default value of 10% has been used. Reprinted figure with permission from [37].

atmospheric neutrinos, mainly multi-GeV e-like events, are sensitive to the neutrino mass hierarchy if θ_{13} is sufficiently large due to Earth matter effects, whilst sub-GeV e-like events provide sensitivity to the octant of θ_{23} due to oscillations with Δm^2_{21}.

The result of running during 5 years in neutrino mode for SPL and Beta Beam, adding further the atmospheric neutrino data, is shown in Fig. 24 [37]. One can appreciate that practically all degeneracies can be eliminated as only the solution with the wrong sign survives with a $\Delta\chi^2 = 3.3$. This last degeneracy can be completely eliminated by using a neutrino running mode combined with anti-neutrino mode and ATM data [37]. However, the example shown is a favorable case with $\sin^2\theta_{23} = 0.6$ and in general, for $\sin^2\theta_{23} < 0.5$, the impact of the atmospheric data is weaker. So, as a generic case, for the CERN-MEMPHYS project, one is left with the four intrinsic degeneracies. However, the important observation in Fig. 24 is that degeneracies have only a very small impact on the CP violation discovery, in the sense that if the true solution is CP violating also the fake solutions are located at CP violating values of $\delta_{\rm CP}$. Therefore, thanks to the relatively short baseline without matter effect, even if degeneracies affect the precise determination of θ_{13} and $\delta_{\rm CP}$, they have only a small impact on the CP violation discovery potential. Furthermore, one would quote explicitly the four possible sets of parameters with their respective confidential level. It is also clear from the figure that the sign(Δm^2_{31}) degeneracy has practically no effect on the θ_{13} measurement, whereas the octant degeneracy has very little impact on the determination of $\delta_{\rm CP}$.

Some other features of the atmospheric neutrino data are presented in Sec. 7. In order to fully exploit the possibilities offered by a Neutrino Factory, the detector should be capable of identifying and measuring all three charged lepton flavors produced in charged-current interactions and of measuring their charges in order to identify the incoming neutrino helicity. The GLACIER concept in its non-magnetized option provides a background-free identification of electron-neutrino charged-current events and a kinematical selection of tau-neutrino charged-current interactions. We can assume that charge discrimination is available for muons reaching an external

Table 11. Expected events rates for GLACIER in a Neutrino Factory beam, assuming no oscillations and for 10^{20} muon decays (E_μ=30 GeV). N_{tot} is the total number of events and N_{qe} is the number of quasi-elastic events.

Event rates for various baselines							
		$L = 732$ km		$L = 2900$ km		$L = 7400$ km	
		N_{tot}	N_{qe}	N_{tot}	N_{qe}	N_{tot}	N_{qe}
μ^- 10^{20} decays	ν_μ CC	2260 000	90 400	144 000	5760	22 700	900
	ν_μ NC	673 000	—	41 200	—	6800	—
	$\overline{\nu}_e$ CC	871 000	34 800	55 300	2200	8750	350
	$\overline{\nu}_e$ NC	302 000	—	19 900	—	3000	—
μ^+ 10^{20} decays	$\overline{\nu}_\mu$ CC	1010 000	40 400	63 800	2550	10 000	400
	$\overline{\nu}_\mu$ NC	353 000	—	22 400	—	3500	—
	ν_e CC	1970 000	78 800	129 000	5160	19 800	800
	ν_e NC	579 000	—	36 700	—	5800	—

magnetized-Fe spectrometer.

Another interesting and extremely challenging possibility would consist in magnetizing the whole liquid Argon volume [135, 36]. This set-up would allow the clean classification of events into electrons, right-sign muons, wrong-sign muons and no-lepton categories. In addition, high granularity permits a clean detection of quasi-elastic events, which provide a selection of the neutrino electron helicity by detecting the final state proton, without the need of an electron charge measurement. Table 11 summarizes the expected rates for GLACIER and 10^{20} muon decays at a neutrino factory with stored muons having an energy of 30 GeV [136]. N_{tot} is the total number of events and N_{qe} is the number of quasi-elastic events.

Figure 25 shows the expected sensitivity in the measurement of θ_{13} for a baseline of 7400 km. The maximal sensitivity to θ_{13} is achieved for very small background levels, since one is looking in this case for small signals; most of the information is coming from the clean wrong-sign muon class and from quasi-elastic events. On the other hand, if its value is not too small, for a measurement of θ_{13}, the signal/background ratio could be not so crucial, and also the other event classes can contribute to this measurement.

A Neutrino Factory should aim to over-constrain the oscillation pattern, in order to look for unexpected new physics effects. This can be achieved in global fits of the parameters, where the unitarity of the mixing matrix is not strictly assumed. Using a detector able to identify the τ lepton production via kinematic means, it is possible to verify the unitarity in $\nu_\mu \to \nu_\tau$ and $\nu_e \to \nu_\tau$ transitions.

The study of CP violation in the lepton system probably is the most ambitious goal of an experiment at a Neutrino Factory. Matter effects can mimic CP violation; however, a multi-parameter fit at the right baseline can allow a simultaneous determination of matter and CP violating parameters. To detect CP violation effects, the most favorable choice of neutrino energy E_ν and baseline L is in the region of the first maximum, given by $(L/E_\nu)^{max} \simeq 500$ km/GeV for $|\Delta m^2_{32}| = 2.5 \times 10^{-3}$ eV^2 [137]. To study oscillations in this region, one has to require that the energy of the "first-maximum" be smaller than the MSW resonance energy: $2\sqrt{2}G_F n_e E_\nu^{max} \lesssim \Delta m^2_{32} \cos 2\theta_{13}$. This fixes a limit on the baseline $L_{max} \approx 5000$ km beyond which

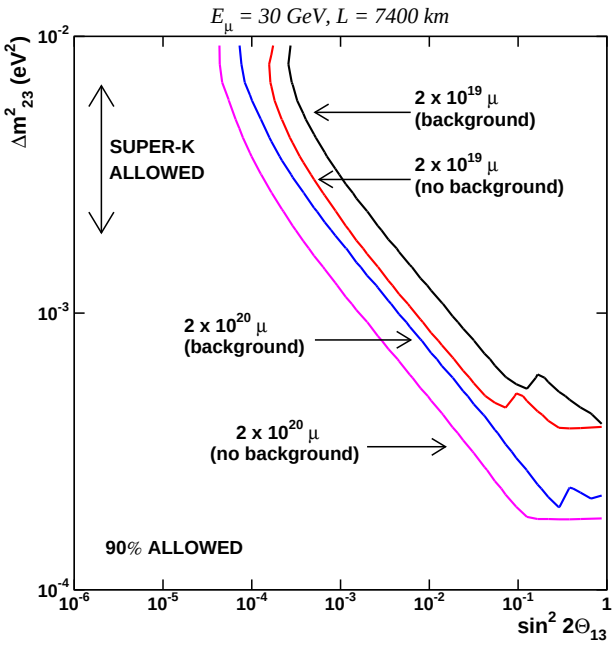

Figure 25. GLACIER sensitivity to the measurement of θ_{13}. Reprinted figure with permission from [136].

matter effects spoil the sensitivity.

As an example, Fig. 26 shows the sensitivity to the CP violating phase δ_{CP} for two concrete cases. The events are classified in the five categories previously mentioned, assuming an electron charge confusion of 0.1%. The exclusion regions in the $\Delta m^2_{12} - \delta_{CP}$ plane are determined by fitting the visible energy distributions, provided that the electron detection efficiency is $\sim 20\%$. The excluded regions extend up to values of $|\delta_{CP}|$ close to π, even when θ_{13} is left free.

12. Conclusions and outlook

In this paper we discuss the importance of outstanding physics phenomena such as the possible instability of matter (proton decay), the production of neutrinos in supernovae, in the Sun and in the interior of the Earth, as well as the recently discovered process of neutrino oscillations, also detectable through artificial neutrinos produced by nuclear reactors and particle accelerators.

All the above physics subjects, key issues for particle physics, astro-particle physics, astrophysics and cosmology, call for a new generation of multipurpose, underground observatories based on improved detection techniques.

The envisioned detectors must necessarily be very massive (and consequently large) and able to provide very low experimental background. The required signal to noise ratio can only be achieved in underground laboratories suitably shielded against cosmic-rays and environmental radioactivity. Some candidate sites in Europe have

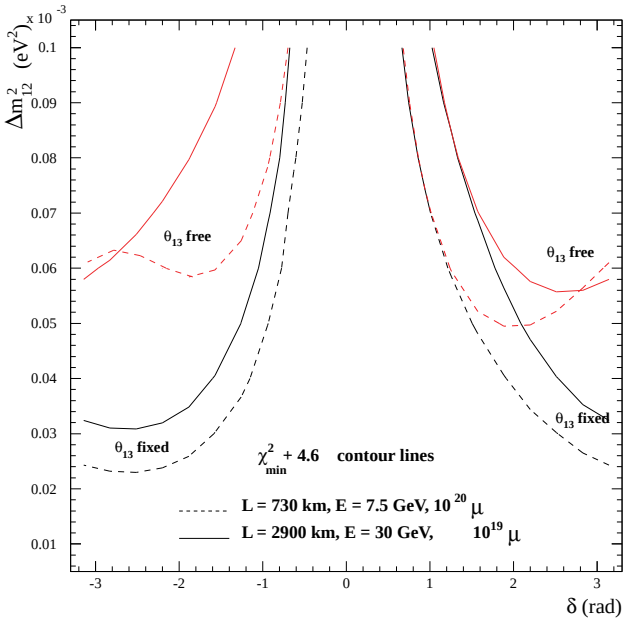

Figure 26. GLACIER 90% C.L. sensitivity on the CP-phase δ_{CP} as a function of Δm^2_{21} for the two considered baselines. In contrast to Fig. 22 only the conserving phase $\delta_{CP} = 0$ is considered and the other reference oscillation parameters are $\Delta m^2_{32} = 3 \times 10^{-3}$ eV^2, $\sin^2\theta_{23} = 0.5$, $\sin^2\theta_{12} = 0.5$ and $\sin^2 2\theta_{13} = 0.05$. The lower curves are made fixing all parameters to the reference values while for the upper curves θ_{13} is free. Reprinted figure with permission from [137].

been identified and we are progressing in assessing in detail their capabilities.

We have identified three different and, to a large extent, complementary technologies capable of meeting the challenge, based on large scale use of liquids for building large-size, volume-instrumented detectors. The three proposed large-mass, liquid-based detectors for future underground observatories for particle physics in Europe (GLACIER, LENA and MEMPHYS), although based on completely different detection techniques (liquid Argon, liquid scintillator and water Cherenkov), share a similar, very rich physics program. For some cases of interest their detection properties are quite complementary. A summary of the scientific case presented in this paper is given for astro-particle physics topics in Table 12.

Acknowledgments

We wish to warmly acknowledge support from all the various funding agencies. We wish to thank the EU framework 6 project ILIAS for providing assistance particularly regarding underground site aspects (contract 8R113-CT-2004-506222).

Table 12. Summary of the physics potential of the proposed detectors for astro-particle physics topics. The (*) stands for the case where Gadolinium salt is added to the water of one of the MEMPHYS shafts.

Topics	GLACIER 100 kton	LENA 50 kton	MEMPHYS 440 kton
Proton decay			
$e^+\pi^0$	0.5×10^{35}	—	1.0×10^{35}
$\bar{\nu}K^+$	1.1×10^{35}	0.4×10^{35}	0.2×10^{35}
SN ν (10 kpc)			
CC	$2.5 \times 10^4(\nu_e)$	$9.0 \times 10^3(\bar{\nu}_e)$	$2.0 \times 10^5(\bar{\nu}_e)$
NC	3.0×10^4	3.0×10^3	—
ES	$1.0 \times 10^3(e)$	$7.0 \times 10^3(p)$	$1.0 \times 10^3(e)$
DSNB ν (S/B 5 years)	40-60/30	9-110/7	43-109/47 (*)
Solar ν (Evts. 1 year)			
^{8}B ES	4.5×10^4	1.6×10^4	1.1×10^5
^{8}B CC	—	360	—
^{7}Be	—	2.0×10^6	—
pep	—	7.7×10^4	—
Atmospheric ν (Evts. 1 year)	1.1×10^4	—	4.0×10^4 (1-ring only)
Geo ν (Evts. 1 year)	below threshold	≈ 1000	need 2 MeV threshold
Reactor ν (Evts. 1 year))	—	1.7×10^4	6.0×10^4 (*)
Dark Matter (Evts. 10 years)	3 events ($\sigma_{ES} = 10^{-4}$,$M > 20$ GeV)	—	—

References

[1] J. C. Pati and A. Salam, "Is Baryon Number Conserved?" *Phys. Rev. Lett.* **31** (1973) 661–664.

[2] P. Nath and P. Fileviez Pérez, "Proton stability in grand unified theories, in strings, and in branes" *Phys. Rept.* **441** (2007) 191–317 [hep-ph/0601023].

[3] **Super-Kamiokande** Collaboration, K. Kobayashi *et. al.*, "Search for nucleon decay via modes favored by supersymmetric grand unification models in Super-Kamiokande-I" *Phys. Rev.* **D72** (2005) 052007 [hep-ex/0502026].

[4] J. Davis, Raymond, D. S. Harmer and K. C. Hoffman, "Search for neutrinos from the sun" *Phys. Rev. Lett.* **20** (1968) 1205–1209.

[5] **Kamiokande-II** Collaboration, K. S. Hirata *et. al.*, "Observation of B-8 solar neutrinos in the Kamiokande-II detector" *Phys. Rev. Lett.* **63** (1989) 16.

[6] **GALLEX** Collaboration, P. Anselmann *et. al.*, "Solar neutrinos observed by GALLEX at Gran Sasso." *Phys. Lett.* **B285** (1992) 376–389.

[7] D. N. Abdurashitov *et. al.*, "Results from SAGE" *Phys. Lett.* **B328** (1994) 234–248.

[8] **Super-Kamiokande** Collaboration, M. B. Smy, "Solar neutrino precision measurements using all 1496 days of Super-Kamiokande-I data" *Nucl. Phys. Proc. Suppl.* **118** (2003) 25–32 [hep-ex/0208004].

[9] **SNO** Collaboration, B. Aharmim *et. al.*, "Electron energy spectra, fluxes, and day-night asymmetries of B-8 solar neutrinos from the 391-day salt phase SNO data set" *Phys. Rev.* **C72** (2005) 055502 [nucl-ex/0502021].

[10] **GNO** Collaboration, M. Altmann *et. al.*, "Complete results for five years of GNO solar neutrino observations" *Phys. Lett.* **B616** (2005) 174–190 [hep-ex/0504037].

[11] **Kamiokande-II** Collaboration, K. Hirata *et. al.*, "Observation of a neutrino burs from the supernova SN1987a" *Phys. Rev. Lett.* **58** (1987) 1490–1493.

[12] R. M. Bionta *et. al.*, "Observation of a neutrino burst in coincidence with supernova SN1987A in the Large Magellanic Clound" *Phys. Rev. Lett.* **58** (1987) 1494.

[13] E. N. Alekseev, L. N. Alekseeva, I. V. Krivosheina and V. I. Volchenko, "Detection of the neutrino signal from SN1987A in the LMC using the INR Baksan underground scintillator telescope" *Phys. Lett.* **B205** (1988) 209–214.

[14] **The NUSEX** Collaboration, M. Aglietta *et. al.*, "Experimental study of atmospheric neutrino flux in the NUSEX experiment" *Europhys. Lett.* **8** (1989) 611–614.

[15] **Kamiokande-II** Collaboration, K. S. Hirata *et. al.*, "Experimental study of the atmospheric neutrino flux" *Phys. Lett.* **B205** (1988) 416.

[16] **Kamiokande-II** Collaboration, K. S. Hirata *et. al.*, "Observation of a small atmospheric ν_μ/ν_e ratio in Kamiokande" *Phys. Lett.* **B280** (1992) 146–152.

[17] R. Becker-Szendy *et. al.*, "The Electron-neutrino and muon-neutrino content of the atmospheric flux" *Phys. Rev.* **D46** (1992) 3720–3724.

[18] **Fréjus** Collaboration, K. Daum *et. al.*, "Determination of the atmospheric neutrino spectra with the Fréjus detector" *Z. Phys.* **C66** (1995) 417–428.

[19] **Soudan-2** Collaboration, W. W. M. Allison *et. al.*, "The atmospheric neutrino flavor ratio from a 3.9 fiducial kiloton-year exposure of Soudan 2" *Phys. Lett.* **B449** (1999) 137–144 [hep-ex/9901024].

[20] **Super-Kamiokande** Collaboration, Y. Ashie *et. al.*, "A measurement of atmospheric neutrino oscillation parameters by Super-Kamiokande I" *Phys. Rev.* **D71** (2005) 112005 [hep-ex/0501064].

[21] **Super-Kamiokande** Collaboration, Y. Fukuda *et. al.*, "Evidence for oscillation of atmospheric neutrinos" *Phys. Rev. Lett.* **81** (1998) 1562–1567 [hep-ex/9807003].

[22] T. Kajita, "Discovery of neutrino oscillations" *Rept. Prog. Phys.* **69** (2006) 1607–1635.

[23] T. Tabarelli de Fatis, "Prospects of measuring $sin^2(2\theta_{13})$ and the sign of Δm^2 with a massive magnetized detector for atmospheric neutrinos" *Eur. Phys. J.* **C24** (2002) 43–50 [hep-ph/0202232].

[24] T. Araki *et. al.*, "Experimental investigation of geologically produced antineutrinos with KamLAND" *Nature* **436** (2005) 499–503.

[25] **Borexino** Collaboration, H. O. Back *et. al.*, "Phenylxylylethane (PXE): A high-density, high-flashpoint organic liquid scintillator for applications in low-energy particle and astrophysics experiments" physics/0408032.

[26] **KamLAND** Collaboration, T. Araki *et. al.*, "Measurement of neutrino oscillation with KamLAND: Evidence of spectral distortion" *Phys. Rev. Lett.* **94** (2005) 081801 [hep-ex/0406035].

[27] **ICARUS** Collaboration, S. Amerio *et. al.*, "Design, construction and tests of the ICARUS

T600 detector" *Nucl. Instrum. Meth.* **A527** (2004) 329–410.
[28] **ICARUS** Collaboration, F. Arneodo *et. al.*, "The ICARUS experiment, a second-generation proton decay experiment and neutrino observatory at the Gran Sasso Laboratory" hep-ex/0103008.
[29] A. de Bellefon *et. al.*, "MEMPHYS: A large scale water Cherenkov detector at Fréjus" hep-ex/0607026.
[30] L. Oberauer, F. von Feilitzsch and W. Potzel, "A large liquid scintillator detector for low-energy neutrino astronomy" *Nucl. Phys. Proc. Suppl.* **138** (2005) 108–111.
[31] T. Marrodán Undagoitia *et. al.*, "Low energy neutrino astronomy with the large liquid scintillator detector LENA" *Prog. Part. Nucl. Phys.* **57** (2006) 283 [hep-ph/0605229].
[32] A. Rubbia, "Experiments for CP-violation: A giant liquid argon scintillation, Cherenkov and charge imaging experiment?" hep-ph/0402110.
[33] A. Rubbia, "Review of massive underground detectors" hep-ph/0407297.
[34] A. Ereditato and A. Rubbia, "Ideas for future liquid argon detectors" *Nucl. Phys. Proc. Suppl.* **139** (2005) 301–310 [hep-ph/0409143].
[35] A. Ereditato and A. Rubbia, "The liquid argon TPC: A powerful detector for future neutrino experiments and proton decay searches" *Nucl. Phys. Proc. Suppl.* **154** (2006) 163–178 [hep-ph/0509022].
[36] A. Ereditato and A. Rubbia, "Conceptual design of a scalable multi-kton superconducting magnetized liquid argon TPC" *Nucl. Phys. Proc. Suppl.* **155** (2006) 233–236 [hep-ph/0510131].
[37] J. E. Campagne, M. Maltoni, M. Mezzetto and T. Schwetz, "Physics potential of the CERN-MEMPHYS neutrino oscillation project" *JHEP* **04** (2007) 003 [hep-ph/0603172].
[38] C. Rubbia, A. Ferrari, Y. Kadi and V. Vlachoudis, "Beam cooling with ionisation losses" hep-ph/0602032.
[39] K. S. Hirata *et. al.*, "Observation in the Kamiokande-II detector of the neutrino burst from supernova SN1987A" *Phys. Rev.* **D38** (1988) 448–458.
[40] M. Wurm *et. al.*, "Detection potential for the diffuse supernova neutrino background in the large liquid-scintillator detector LENA" *Phys. Rev.* **D75** (2007) 023007 [astro-ph/0701305].
[41] J. F. Beacom and M. R. Vagins, "GADZOOKS! Antineutrino spectroscopy with large water Cherenkov detectors" *Phys. Rev. Lett.* **93** (2004) 171101 [hep-ph/0309300].
[42] I. Dorsner and P. Fileviez Pérez, "How long could we live?" *Phys. Lett.* **B625** (2005) 88–95 [hep-ph/0410198].
[43] H. Georgi and S. L. Glashow, "Unity of all elementary particle forces" *Phys. Rev. Lett.* **32** (1974) 438–441.
[44] I. Dorsner and P. Fileviez Pérez, "Unification without supersymmetry: Neutrino mass, proton decay and light leptoquarks" *Nucl. Phys.* **B723** (2005) 53–76 [hep-ph/0504276].
[45] I. Dorsner, P. Fileviez Pérez and R. Gonzalez Felipe, "Phenomenological and cosmological aspects of a minimal GUT scenario" *Nucl. Phys.* **B747** (2006) 312–327 [hep-ph/0512068].
[46] D.-G. Lee, R. N. Mohapatra, M. K. Parida and M. Rani, "Predictions for proton lifetime in minimal nonsupersymmetric SO(10) models: An update" *Phys. Rev.* **D51** (1995) 229–235 [hep-ph/9404238].
[47] H. Murayama and A. Pierce, "Not even decoupling can save minimal supersymmetric SU(5)" *Phys. Rev.* **D65** (2002) 055009 [hep-ph/0108104].
[48] B. Bajc, P. Fileviez Perez and G. Senjanovic, "Proton decay in minimal supersymmetric SU(5)" *Phys. Rev.* **D66** (2002) 075005 [hep-ph/0204311].
[49] B. Bajc, P. Fileviez Perez and G. Senjanovic, "Minimal supersymmetric SU(5) theory and proton decay: Where do we stand?" hep-ph/0210374.
[50] D. Emmanuel-Costa and S. Wiesenfeldt, "Proton decay in a consistent supersymmetric SU(5) GUT model" *Nucl. Phys.* **B661** (2003) 62–82 [hep-ph/0302272].
[51] K. S. Babu and R. N. Mohapatra, "Predictive neutrino spectrum in minimal SO(10) grand unification" *Phys. Rev. Lett.* **70** (1993) 2845–2848 [hep-ph/9209215].
[52] C. S. Aulakh, B. Bajc, A. Melfo, G. Senjanovic and F. Vissani, "The minimal supersymmetric grand unified theory" *Phys. Lett.* **B588** (2004) 196–202 [hep-ph/0306242].
[53] T. Fukuyama, A. Ilakovac, T. Kikuchi, S. Meljanac and N. Okada, "Detailed analysis of proton decay rate in the minimal supersymmetric SO(10) model" *JHEP* **09** (2004) 052 [hep-ph/0406068].
[54] H. S. Goh, R. N. Mohapatra, S. Nasri and S.-P. Ng, "Proton decay in a minimal SUSY SO(10) model for neutrino mixings" *Phys. Lett.* **B587** (2004) 105–116 [hep-ph/0311330].
[55] T. Friedmann and E. Witten, "Unification scale, proton decay, and manifolds of G(2)

holonomy" *Adv. Theor. Math. Phys.* **7** (2003) 577–617 [hep-th/0211269].
[56] B. Bajc and G. Senjanovic, "Seesaw at LHC" hep-ph/0612029.
[57] P. Fileviez Perez, "Renormalizable Adjoint SU(5)" hep-ph/0702287.
[58] A. Bueno *et. al.*, "Nucleon decay searches with large liquid argon TPC detectors at shallow depths: Atmospheric neutrinos and cosmogenic backgrounds" *JHEP* **04** (2007) [hep-ph/0701101].
[59] **GEANT4** Collaboration, S. Agostinelli *et. al.*, "GEANT4: A simulation toolkit" *Nucl. Instrum. Meth.* **A506** (2003) 250–303.
[60] T. Marrodán Undagoitia *et. al.*, "Search for the proton decay $p \leftarrow K^+ + \bar{\nu}$ in the large liquid scintillator low energy neutrino astronomy detector LENA" *Phys. Rev.* **D72** (2005) 075014 [hep-ph/0511230].
[61] C. K. Jung, "Feasibility of a next generation underground water Cherenkov detector: UNO" *AIP Conf. Proc.* **533** (2000) 29–34 [hep-ex/0005046].
[62] T. Nakaya, "Next-generation nucleon decay experiments" *Nucl. Phys. Proc. Suppl.* **138** (2005) 376–382.
[63] A. S. Dighe and A. Y. Smirnov, "Identifying the neutrino mass spectrum from the neutrino burst from a supernova" *Phys. Rev.* **D62** (2000) 033007 [hep-ph/9907423].
[64] M. Aglietta *et. al.*, "Comments on the two events observed in neutrino detectors during the supernova 1987a outburst" *Europhys. Lett.* **3** (1987) 1321–1324.
[65] L. Cadonati, F. P. Calaprice and M. C. Chen, "Supernova neutrino detection in Borexino" *Astropart. Phys.* **16** (2002) 361–372 [hep-ph/0012082].
[66] J. F. Beacom, W. M. Farr and P. Vogel, "Detection of supernova neutrinos by neutrino proton elastic scattering" *Phys. Rev.* **D66** (2002) 033001 [hep-ph/0205220].
[67] M. Kachelriess *et. al.*, "Exploiting the neutronization burst of a galactic supernova" *Phys. Rev.* **D71** (2005) 063003 [astro-ph/0412082].
[68] I. Gil-Botella and A. Rubbia, "Decoupling supernova and neutrino oscillation physics with LAr TPC detectors" *JCAP* **0408** (2004) 001 [hep-ph/0404151].
[69] I. Gil-Botella and A. Rubbia, "Oscillation effects on supernova neutrino rates and spectra and detection of the shock breakout in a liquid argon TPC" *JCAP* **0310** (2003) 009 [hep-ph/0307244].
[70] R. C. Schirato and G. M. Fuller, "Connection between supernova shocks, flavor transformation, and the neutrino signal" astro-ph/0205390.
[71] G. L. Fogli, E. Lisi, D. Montanino and A. Mirizzi, "Analysis of energy- and time-dependence of supernova shock effects on neutrino crossing probabilities" *Phys. Rev.* **D68** (2003) 033005 [hep-ph/0304056].
[72] G. L. Fogli, E. Lisi, A. Mirizzi and D. Montanino, "Probing supernova shock waves and neutrino flavor transitions in next-generation water-Cherenkov detectors" *JCAP* **0504** (2005) 002 [hep-ph/0412046].
[73] R. Tomas *et. al.*, "Neutrino signatures of supernova shock and reverse shock propagation" *JCAP* **0409** (2004) 015 [astro-ph/0407132].
[74] V. Barger, P. Huber and D. Marfatia, "Supernova neutrinos can tell us the neutrino mass hierarchy independently of flux models" *Phys. Lett.* **B617** (2005) 167–173 [hep-ph/0501184].
[75] G. L. Fogli, E. Lisi, A. Mirizzi and D. Montanino, "Damping of supernova neutrino transitions in stochastic shock-wave density profiles" *JCAP* **0606** (2006) 012 [hep-ph/0603033].
[76] A. Friedland and A. Gruzinov, "Neutrino signatures of supernova turbulence" astro-ph/0607244.
[77] C. Lunardini and A. Y. Smirnov, "Supernova neutrinos: Earth matter effects and neutrino mass spectrum" *Nucl. Phys.* **B616** (2001) 307–348 [hep-ph/0106149].
[78] G. L. Fogli, E. Lisi, D. Montanino and A. Palazzo, "Supernova neutrino oscillations: A simple analytical approach" *Phys. Rev. D* **65** (Mar, 2002) 073008.
[79] G. L. Fogli, E. Lisi, D. Montanino and A. Palazzo, "Erratum: Supernova neutrino oscillations: A simple analytical approach [Phys. Rev. D 65, 073008 (2002)]" *Phys. Rev. D* **66** (Aug, 2002) 039901.
[80] A. S. Dighe, M. T. Keil and G. G. Raffelt, "Identifying earth matter effects on supernova neutrinos at a single detector" *JCAP* **0306** (2003) 006 [hep-ph/0304150].
[81] A. S. Dighe, M. T. Keil and G. G. Raffelt, "Detecting the neutrino mass hierarchy with a supernova at IceCube" *JCAP* **0306** (2003) 005 [hep-ph/0303210].
[82] A. Mirizzi, G. G. Raffelt and P. D. Serpico, "Earth matter effects in supernova neutrinos: Optimal detector locations" *JCAP* **0605** (2006) 012 [astro-ph/0604300].
[83] H. Duan, G. M. Fuller, J. Carlson and Y.-Z. Qian, "Simulation of coherent non-linear neutrino

flavor transformation in the supernova environment. I: Correlated neutrino trajectories" *Phys. Rev.* **D74** (2006) 105014 [astro-ph/0606616].
[84] S. Hannestad, G. G. Raffelt, G. Sigl and Y. Y. Y. Wong, "Self-induced conversion in dense neutrino gases: Pendulum in flavour space" *Phys. Rev.* **D74** (2006) 105010 [astro-ph/0608695].
[85] G. G. Raffelt and A. Y. Smirnov, "Self-induced spectral splits in supernova neutrino fluxes" arXiv:0705.1830 [hep-ph].
[86] R. Tomas, D. Semikoz, G. G. Raffelt, M. Kachelriess and A. S. Dighe, "Supernova pointing with low- and high-energy neutrino detectors" *Phys. Rev.* **D68** (2003) 093013 [hep-ph/0307050].
[87] P. Antonioli *et. al.*, "SNEWS: The SuperNova Early Warning System" *New J. Phys.* **6** (2004) 114 [astro-ph/0406214].
[88] A. Odrzywolek, M. Misiaszek and M. Kutschera, "Detection possibility of the pair-annihilation neutrinos from the neutrino-cooled pre-supernova star" *Astropart. Phys.* **21** (2004) 303–313 [astro-ph/0311012].
[89] S. Ando, J. F. Beacom and H. Yuksel, "Detection of neutrinos from supernovae in nearby galaxies" *Phys. Rev. Lett.* **95** (2005) 171101 [astro-ph/0503321].
[90] M. Fukugita and M. Kawasaki, "Constraints on the star formation rate from supernova relic neutrino observations" *Mon. Not. Roy. Astron. Soc.* **340** (2003) L7 [astro-ph/0204376].
[91] S. Ando, "Cosmic star formation history and the future observation of supernova relic neutrinos" *Astrophys. J.* **607** (2004) 20–31 [astro-ph/0401531].
[92] S. Ando, "Decaying neutrinos and implications from the supernova relic neutrino observation" *Phys. Lett.* **B570** (2003) 11 [hep-ph/0307169].
[93] G. L. Fogli, E. Lisi, A. Mirizzi and D. Montanino, "Three-generation flavor transitions and decays of supernova relic neutrinos" *Phys. Rev.* **D70** (2004) 013001 [hep-ph/0401227].
[94] **Super-Kamiokande** Collaboration, M. Malek *et. al.*, "Search for supernova relic neutrinos at Super-Kamiokande" *Phys. Rev. Lett.* **90** (2003) 061101 [hep-ex/0209028].
[95] L. E. Strigari, J. F. Beacom, T. P. Walker and P. Zhang, "The concordance cosmic star formation rate: Implications from and for the supernova neutrino and gamma ray backgrounds" *JCAP* **0504** (2005) 017 [astro-ph/0502150].
[96] A. M. Hopkins and J. F. Beacom, "On the normalisation of the cosmic star formation history" *Astrophys. J.* **651** (2006) 142 [astro-ph/0601463].
[97] A. G. Cocco, A. Ereditato, G. Fiorillo, G. Mangano and V. Pettorino, "Supernova relic neutrinos in liquid argon detectors" *JCAP* **0412** (2004) 002 [hep-ph/0408031].
[98] H. Yuksel, S. Ando and J. F. Beacom, "Direct measurement of supernova neutrino emission parameters with a gadolinium enhanced Super-Kamiokande detector" *Phys. Rev.* **C74** (2006) 015803 [astro-ph/0509297].
[99] T. Totani, K. Sato, H. E. Dalhed and J. R. Wilson, "Future detection of supernova neutrino burst and explosion mechanism" *Astrophys. J.* **496** (1998) 216–225 [astro-ph/9710203].
[100] T. A. Thompson, A. Burrows and P. A. Pinto, "Shock breakout in core-collapse supernovae and its neutrino signature" *Astrophys. J.* **592** (2003) 434 [astro-ph/0211194].
[101] M. T. Keil, G. G. Raffelt and H.-T. Janka, "Monte Carlo study of supernova neutrino spectra formation" *Astrophys. J.* **590** (2003) 971–991 [astro-ph/0208035].
[102] **Borexino** Collaboration, G. Alimonti *et. al.*, "Ultra-low background measurements in a large volume underground detector" *Astropart. Phys.* **8** (1998) 141–157.
[103] G. Alimonti *et. al.*, "A large-scale low-background liquid scintillation detector: The counting test facility at Gran Sasso" *Nucl. Instrum. Meth.* **A406** (1998) 411–426.
[104] A. Ianni, D. Montanino and F. L. Villante, "How to observe B-8 solar neutrinos in liquid scintillator detectors" *Phys. Lett.* **B627** (2005) 38–48 [physics/0506171].
[105] T. Hagner *et. al.*, "Muon induced production of radioactive isotopes in scintillation detectors" *Astropart. Phys.* **14** (2000) 33–47.
[106] H. Back *et. al.*, "CNO and pep neutrino spectroscopy in Borexino: Measurement of the deep-underground production of cosmogenic C11 in an organic liquid scintillator" *Phys. Rev.* **C74** (2006) 045805.
[107] M. C. Gonzalez-Garcia and Y. Nir, "Developments in neutrino physics" *Rev. Mod. Phys.* **75** (2003) 345–402 [hep-ph/0202058].
[108] **MACRO** Collaboration, M. Ambrosio *et. al.*, "Matter effects in upward-going muons and sterile neutrino oscillations" *Phys. Lett.* **B517** (2001) 59–66 [hep-ex/0106049].
[109] **K2K** Collaboration, M. H. Ahn *et. al.*, "Measurement of neutrino oscillation by the K2K experiment" hep-ex/0606032.
[110] **MINOS** Collaboration, N. Tagg, "First MINOS results from the NuMI beam" *ECONF*

C060409 (2006) 019 [hep-ex/0605058].
[111] Y. Itow *et. al.*, "The JHF-Kamioka neutrino project" hep-ex/0106019.
[112] **NOvA** Collaboration, D. S. Ayres *et. al.*, "NOvA proposal to build a 30-kiloton off-axis detector to study neutrino oscillations in the Fermilab NuMI beamline" hep-ex/0503053.
[113] P. Huber, M. Maltoni and T. Schwetz, "Resolving parameter degeneracies in long-baseline experiments by atmospheric neutrino data" *Physical Review D* **71** (2005) 053006.
[114] C. W. Kim and U. W. Lee, "Comment on the possible electron-neutrino excess in the Super-Kamiokande atmospheric neutrino experiment" *Phys. Lett.* **B444** (1998) 204–207 [hep-ph/9809491].
[115] O. L. G. Peres and A. Y. Smirnov, "Testing the solar neutrino conversion with atmospheric neutrinos" *Phys. Lett.* **B456** (1999) 204–213 [hep-ph/9902312].
[116] M. C. Gonzalez-Garcia and M. Maltoni, "Atmospheric neutrino oscillations and new physics" *Phys. Rev.* **D70** (2004) 033010 [hep-ph/0404085].
[117] K. A. Hochmuth *et. al.*, "Probing the Earth's interior with a large-volume liquid scintillator detector" *Astropart. Phys.* **27** (2007) 21–29 [hep-ph/0509136].
[118] A. Bueno, R. Cid, S. Navas-Concha, D. Hooper and T. J. Weiler, "Indirect detection of dark matter WIMPs in a Liquid Argon TPC" *JCAP* **0501** (2005) 001 [hep-ph/0410206].
[119] S. T. Petcov and T. Schwetz, "Precision measurement of solar neutrino oscillation parameters by a long-baseline reactor neutrino experiment in Europe" *Phys. Lett.* **B642** (2006) 487–494 [hep-ph/0607155].
[120] S. Choubey and S. T. Petcov, "Reactor anti-neutrino oscillations and gadolinium loaded Super-Kamiokande detector" *Phys. Lett.* **B594** (2004) 333–346 [hep-ph/0404103].
[121] M. Ishitsuka, T. Kajita, H. Minakata and H. Nunokawa, "Resolving neutrino mass hierarchy and CP degeneracy by two identical detectors with different baselines" *Phys. Rev.* **D72** (2005) 033003 [hep-ph/0504026].
[122] **OPERA** Collaboration, R. Acquafredda *et. al.*, "First events from the CNGS neutrino beam detected in the OPERA experiment" *New J. Phys.* **8** (2006) 303 [hep-ex/0611023].
[123] A. Meregaglia and A. Rubbia, "Neutrino oscillation physics at an upgraded CNGS with large next generation liquid argon TPC detectors" *JHEP* **11** (2006) 032 [hep-ph/0609106].
[124] M. Maltoni, T. Schwetz, M. A. Tortola and J. W. F. Valle, "Status of global fits to neutrino oscillations" *New J. Phys.* **6** (2004) 122 [hep-ph/0405172].
[125] F. Gerigk *et. al.*, "Conceptual design of the SPL II, a high-power superconducting H- linac at CERN". CERN-2006-006.
[126] **BENE Steering Group** Collaboration, A. Baldini *et. al.*, "Beams for European Neutrino Experiments (BENE): Midterm scientific report".
[127] **International Scoping Study** Collaboration, P. Dornan *et. al. in preparation* (2006).
[128] M. G. Catanesi *et. al.*, "Proposal for hadron production measurements using the NA49 detector for use in long-baseline and atmospheric neutrino flux calculations". CERN-SPSC-2001-017.
[129] P. Zucchelli, "A novel concept for a $\bar{\nu}_e/\nu_e$ neutrino factory: The beta beam" *Phys. Lett.* **B532** (2002) 166–172.
[130] J. Bernabeu, J. Burguet-Castell, C. Espinoza and M. Lindroos, "Monochromatic neutrino beams" *JHEP* **12** (2005) 014 [hep-ph/0505054].
[131] J. Sato, "Monoenergetic neutrino beam for long baseline experiments" *Phys. Rev. Lett.* **95** (2005) 131804 [hep-ph/0503144].
[132] J. Burguet-Castell, M. B. Gavela, J. J. Gomez-Cadenas, P. Hernandez and O. Mena, "On the measurement of leptonic CP violation" *Nucl. Phys.* **B608** (2001) 301–318 [hep-ph/0103258].
[133] H. Minakata and H. Nunokawa, "Exploring neutrino mixing with low energy superbeams" *JHEP* **10** (2001) 001 [hep-ph/0108085].
[134] G. L. Fogli and E. Lisi, "Tests of three-flavor mixing in long-baseline neutrino oscillation experiments" *Phys. Rev.* **D54** (1996) 3667–3670 [hep-ph/9604415].
[135] A. Badertscher, M. Laffranchi, A. Meregaglia, A. Muller and A. Rubbia, "First results from a liquid argon time projection chamber in a magnetic field" *Nucl. Instrum. Meth.* **A555** (2005) 294–309 [physics/0505151].
[136] A. Bueno, M. Campanelli and A. Rubbia, "Physics potential at a neutrino factory: Can we benefit from more than just detecting muons?" *Nucl. Phys.* **B589** (2000) 577–608 [hep-ph/0005007].
[137] A. Bueno, M. Campanelli, S. Navas-Concha and A. Rubbia, "On the energy and baseline optimization to study effects related to the delta-phase (CP-T-violation) in neutrino oscillations at a neutrino factory" *Nucl. Phys.* **B631** (2002) 239–284 [hep-ph/0112297].